SKI Report 96:74

# Coupled Transport/Reaction Model of the Properties of Bentonite Buffer in a Repository

Jinsong Liu and Ivars Neretnieks

November 1996

ISSN 1104-1374
ISRN SKI-R--96/74--SE

SKI
STATENS KÄRNKRAFTINSPEKTION
Swedish Nuclear Power Inspectorate

SKI Report 96:74

# Coupled Transport/Reaction Model of the Properties of Bentonite Buffer in a Repository

Jinsong Liu and Ivars Neretnieks

Department of Chemical Engineering and Technology,
Division of Chemical Engineering, Royal Institute of Technology,
100 44 Stockholm, Sweden

November 1996

SKI Order Number 95218

# List of Contents

## Summary

Two mechanisms that can affect the long-term properties of the bentonite buffer surrounding the canister in a final repository of spent nuclear fuel are studied. The two mechanisms are the oxidation of reducing minerals in the buffer by radiolytically generated oxidant, and the low-temperature alteration of Na-montmorillonite in the bentonite buffer to illite. A coupled mass transport with geochemical reaction model is used.

Four cases have been considered, which differ in the assumptions of whether the radiolytically generated oxidant first oxidises uraninite in the spent fuel, or it is directly transported to the bentonite to oxidise the pyrite. The cases also differ in the assumptions of varying initial concentrations of pyrite in the bentonite buffer.

The modelling results show that, at low temperatures, the sodium montmorillonite in the bentonite buffer is chemically stable with respect to the chemical conditions of the near-field. Alteration to illite and thus an increase in hydraulic conductivity and loss of swelling ability is not likely to occur. The radiolytically generated oxidant can possibly oxidise the reducing minerals in the bentonite buffer. A redox front can be generated. In all the cases considered in this study, the modelling results indicate that slightly less than 1% by weight of pyrite in the bentonite buffer will be able to ensure that the redox front does not penetrate through the bentonite buffer within 1 million years.

# 1 Introduction

The Swedish concept for the final disposal of nuclear waste is a multi-barrier system with a canister surrounded by a bentonite buffer disposed in crystalline bedrock at a depth of about 500 m (KBS-3, 1983; SKI, 1991). The long-term properties of the bentonite buffer are of great importance for effective isolation of radionuclides and fission products in the spent fuel.

The isolation properties of the bentonite buffer depend on several specific features of the bentonite. The bentonite contains small amounts of sulphides (mainly in the form of pyrite) and residue organics. The pyrite and organics function as redox buffering material to ensure a reducing environment in the vicinity of the canister. In a reducing environment, solubilities of most of the radionuclides in groundwater are extremely low. Their release by the flow of groundwater and the diffusion in groundwater will thus be very slow. Sorption capacity of the clay material in bentonite will be much higher under reducing conditions than under oxidising conditions.

The major compositional mineral of bentonite is smectite, of which montmorillonite is a variety. Montmorillonite has the crystal structure of the type of layered silicate (phyllosilicate), with each layer formed by an alumino-octahedral sheet sandwiched in two silico-tetrahedral sheets. The interlayer sites are occupied by cations and $H_2O$ (Newman and Brown, 1987). The interlamellar water gives the compacted bentonite a very large swelling capacity when contacted with water. The pores and fractures that are left in the compacted bentonite will mostly be sealed after swelling. Hydraulic conductivity becomes very low. There is almost no groundwater flow through the bentonite.

In addition to the interlamellar cations like $Na^+$, $K^+$, $Ca^{+2}$ and/or $Mg^{+2}$, both the tetrahedral and octahedral sheets of montmorillonite contain OH groups at the sheet surfaces, which under neutral to alkaline conditions can be deprotonised to give the sheet extra negative charges. These negatively-charged sites have a large tendency to bind cations. The sorption capacity of the compacted bentonite is quite high, with a cation exchange capacity (CEC) on the order of 100 meq/100g. Many released radionuclides from the canister will first be sorbed onto the clay material in the bentonite.

Several mechanisms can be envisaged to possibly change the long-term properties and thus degrade the isolation properties of the bentonite buffer. The first one is the oxidation mechanism. Atmospheric oxygen is unlikely to penetrate into the depth of a repository (KBS-3, 1983). Oxygen entrapped in the deposition hole during the construction of the repository is small and will either be depleted by reaction with the reducing components in the near-field, or escape by mass transport, mainly diffusion (Wersin et al., 1994). Radiolytically generated oxidants can, however, last for a longer time and possibly react with (oxidise) the pyrite and the organics in the bentonite either directly, or by first oxidising uraninite in the spent fuel to release hexa-valent uranium as an oxidant. The radiolytically generated oxidant will not be released until the canister is damaged. The canister can possibly last for a time much longer than 1 million years (SKB 91, 1992;

SKI, 1991). Even under rigorous quality control, there could, however, still be a small probability that manufacturing leaves defect welding, a small hole or a crack in the canister wall, and oxidant generated by water radiolysis can escape through it.

Another mechanism that affects the long-term properties of bentonite is the alteration to other minerals. Montmorillonite in the bentonite buffer can be converted to non-expanding hydrous mica (typically illite) (Pusch et al., 1991). The conversion yields a dramatic drop in swelling pressure and stiffness and an increase in hydraulic conductivity (Pusch and Börgesson, 1992). There are two kinds of conversion: high-temperature beidellitisation and low-temperature dissolution alteration. In a final repository, the maximum temperature is about 80°C (KBS-3, 1983; SKI, 1991), the beidellitisation is not likely to occur. The dissolution alteration, however, must be considered.

The third mechanism is the ion-exchange mechanism. The bentonite used in the buffer material will be Na-bentonite. Sodium cations incorporated in the interlamellar sites of montmorillonite can be replaced by calcium cations through cation-exchange. Some investigations showed that this mechanism does not significantly alter the physical properties of smectite buffer of high density (Pusch, 1982). In Project-90 (SKI, 1991), however, the ion exchange of sodium for calcium is considered to be probably the most important chemical alteration of the bentonite buffer, resulting in a loss of plasticity and, to a limited extent, of swelling ability.

The oxidation mechanism has been studied by Romero et al. (1995). The model calculation was based on mass balance of the reducing capacity of the bentonite clay and the diffusive mass transport of the radiolytically generated oxidant through the clay. Detailed chemical reactions have not been considered. Studies of chemical reactions of bentonite with groundwater in the literature have been limited to several specific types of reactions. Kinetics of chemical reactions of the oxidation mechanism has been considered by some authors (Wersin et al., 1994). It has been applied to study the time evolution of entrapped oxygen concentration and redox conditions in the bentonite buffer after the repository is sealed. Effect of radiolysis has not been considered in that study.

In SKI's site specific performance assessment program, a computer program named CALIBRE has been used (Worgan and Robinson, 1995). It models the release and transport of radionuclides from a failed waste-package container, through the surrounding near-field. The detailed geochemical reactions has not, however, been included in the program. Other studies of the near-field chemistry in SKI's SITE-94 project use a reaction path model to evaluate the progress of the reactions between the solid phases and the aqueous phase. The program used was EQ3/6 (Wolery, 1992). The effect of mass transport on the evolution path, however, has not be included (Arthur and Apted, 1994).

Mechanisms of the conversion of montmorillonite to beidellite or illite have been discussed in the literature (e.g. Forslind and Jacobsson, 1975; Pytte, 1982; Push et al., 1991). Most of these studies concentrated on the hydrothermal alteration of montmorillonite to beidellite at high temperatures. By using an Arrehnius-type kinetic relation, Pytte (1982) has extrapolated the conversion rate to low temperatures down to

30°C. At 30°C, the montmorillonite will be stable up to $10^8$ to $10^9$ years according to this model. The kinetic relation accounts only for the ratio of potassium to sodium ion concentrations. How the supply of potassium ions to the system affects the alteration rate has not been considered.

A thermodynamic cation exchange model for bentonite-groundwater interaction has been proposed (Wanner et al., 1992). In that model, only cation exchange reactions have been considered. Other reactions like aqueous phase speciation and dissolution/precipitation of minerals are not included. An ion exchange model has also been used to predict the sorption distribution coefficient of some radionuclides on the bentonite clay (Wanner et al., 1994).

In this report, the long-term properties of the bentonite buffer are studies by coupled mass transport with geochemical reaction model. The model takes into consideration the radiolytic generation of oxidants in the canister, the escape of the oxidants through a small hole on the canister wall, and the diffusion of them into the bentonite buffer. These oxidants can react with reducing minerals in the buffer. A redox front can propagate along the buffer toward the granitic bedrock.

The model also accounts for the diffusive transport of dissolved species in the groundwater in granitic bedrock fractures into the bentonite buffer. These species react with clay minerals in the buffer. If both mass transport and chemical reactions favour the alteration of montmorillonite to illite, illite might be formed. The results obtained by the model, however, indicate that alteration does not occur under the geochemical conditions assumed in the model.

# 2 Theoretical background

## 2.1 Water radiolysis by nuclear radiation energy

There are typically three types of nuclear radiation in the spent fuel within the canister. They are alpha-, beta- and gamma-radiation. The radiation energy is emitted only from radioactive sources, like radionuclides and fission products in the spent fuel. The radiation energy can be deposited in water in the cracks and fissures of the spent fuel. The irradiated water decomposes into reductant (mainly hydrogen molecules) and oxidants, such as oxygen, hydrogen peroxide and some oxidising radicals. This process is called water radiolysis. The generated hydrogen is chemically relatively less reactive and can readily be released out of the system. The oxidants left can potentially oxidise the uranium oxide and other reducing species in the spent fuel, as well as the reducing minerals in the bentonite buffer when the oxidants are released out of the canister.

The radiation energy decreases as the distance from the radiation source increases. For an alpha particle with an initial kinetic energy of 5 MeV ($8.0 \cdot 10^{-13}$ J), the penetration depth is about 40 μm in water and about 10 μm in solids. Beta- and gamma-radiation can usually penetrate centimetres and millimetres in water and solids, respectively (Choppin

and Rydberg, 1980). The presence of beta-radiation decreases the yield of hydrogen due to the higher concentration of radicals from such radiation. Recombination of the oxidant and the reductant takes place to a considerable extent in such case (Christensen and Bjergbakke, 1982). When the groundwater has penetrated into the canister (due to whatever type of canister failure), the more densely ionising alpha-radiation can play an important role.

## 2.2 Oxidation of pyrite

The bentonite buffer will contain certain amounts of reducing iron minerals like pyrite. After the sealing of the repository and the transient period has passed, the only conceivable source of oxidant to oxidise the pyrite is the radiolytically generated oxidant.

Oxidation of pyrite is characterised by the following reactions (Stumm and Morgan, 1996): (1) the oxidation of sulphide in the pyrite to sulphate, releasing dissolved ferrous iron and acidity into the water; (2) oxidation of the dissolved ferrous iron to ferric iron; (3)hydrolysis the ferric iron to form insoluble ferric hydroxide, releasing more acidity to the water; (4) reduction of ferric iron by pyrite itself. The rate determining step is the oxidation of Fe(II) to Fe(III), usually catalysed by autotrophic bacteria (Singer and Stumm, 1970).

In the present model of this report, detailed bacterium-mediated kinetics is not considered. Minerals are assumed to be in equilibrium with respect to the aqueous phase. Mineral dissolution is controlled by the solubility and mass transport.

## 2.3 Alteration of montmorillonite and loss of swelling ability

Montmorillonite is a phyllosilicate (layer silicate) of the 2:1 group clay minerals. It swells in water. The swelling, or lack of it, is controlled by the balance of attractive and repulsive forces between adjacent 2:1 layers. The main attractive force is the electrostatic interaction between the negatively charged layers and the positively charged interlayer cations. The main repulsive force arises from the solvation (hydration when it is in water) of interlayer cations as well as from the interaction of the solvate with the surface oxygen of the 2:1 layers (Newman and Brown, 1987).

The uptake of water between the aluminosilicate layers of swelling clay minerals differs in important respects from the sorption of water on free external surfaces. The interlayer cations are hydrated with the interlayer water. The hydrating water is arranged in a partly ordered structure around the interlayer cations. The hydration provides the driving force for expansion. (Newman, 1987).

Illite is a 2:1 group, mica-like clay mineral. It differs from montmorillonite in that it contains relatively more interlayer potassium cations than montmorillonite. Its swelling ability is much less than that of montmorillonite. Beidellite are distinguished from

montmorillonite on the basis of the site of the negative charge on the layers. In montmorillonite, the charge arises from divalent cation substitution in the octahedral sites, whereas in beidellite it arises from the substitution of $Al^{+3}$ in the tetrahedral sites (Newman and Brown, 1987). Beidellite is also less swelling than montmorillonite.

Montmorillonite can possibly be converted to non-swelling hydrous micas. At high temperatures (above 130°C), the tetrahedrally co-ordinated silicon may be replaced by aluminium, the charge balance is then made by uptake of external potassium and release of sodium. It goes through a solid solution mechanism, by forming mixtures of hydrous mica flakes with the unaltered montmorillonite flakes. The ultimate resulting mineral is beidellite. The alteration is often termed beidellitisation. At relatively low temperatures (below 130°C), montmorillonite dissolves in aqueous solution, at the same time new phase of hydrous mica is formed in the voids of the smectite clay phase. Silicon and aluminium or magnesium are supplied by the dissolution, while potassium enters from outside and triggers crystallisation of hydrous mica (Pusch et al., 1991). The resulting mineral is illite. Both processes lead to the formation (or successive formation) of hydrous mica (Push et al., 1991). The conversion from montmorillonite to hydrous mica yields a dramatic drop in swelling pressure and stiffness and an increase in hydraulic conductivity (Pusch and Börgesson, 1992). In this study, only the low-temperature alteration to illite is concerned since the maximum temperature expected is 80°C in the near-field of a repository.

# 3 The coupled mass transport with geochemical reaction modelling

Many programs of coupled transport/reaction models have been developed. All these programs have pros and cons. Many of them have only been demonstrated to work successfully for some highly simplified test problems. Very few of them have been tested in solving real-case, full-scale problems. In this study, the CHEQMATE program (Haworth et al., 1988) is used. This program has been successfully tested in two important natural analogue studies, the natural analogue studies of the Poços de Caldas uranium mine in Brazil (Cross et al., 1991) and the Cigar Lake uranium deposit in Canada (Liu, 1995). The program seems to be quite suitable for modelling geochemical evolution of natural systems. When the program is supplemented with a recently developed time-scaling technique (Liu, 1995; Neretnieks et al., 1995), the prediction can be made for a very long time.

The CHEQMATE (Chemical Equilibrium with Migration and Transport Equations) program (Haworth et al., 1988) has been developed to model the evolution of spatially inhomogeneous geochemical systems. Such systems are characterised by simultaneous chemical-equilibria and the process of mass transport and migration of aqueous species.

For every aqueous species, either simple cations and anions, or dissolved complexes, there is a partial differential equation describing the mass transport of the species in the space domain considered by the program. The domain is usually a natural geological

formation and is often modelled as a porous medium. In one-dimensional rectangular co-ordinate, the mass transport equation for the $j$th aqueous species is

$$\frac{\partial C_j}{\partial t} = D_j \frac{\partial^2 C_j}{\partial x^2} - \frac{1}{\varepsilon} V \frac{\partial C_j}{\partial x} + q_j \tag{3.1}$$

where $C_j$ is the concentration of the $j$th species (mol $m^{-3}$), $D_j$ is the diffusivity of the $j$th species ($m^2$ $s^{-1}$), $\varepsilon$ is the porosity of the domain, $V$ is the groundwater velocity (m $s^{-1}$) and $q_j$ is the source term (mol $m^{-3}$ $s^{-1}$). The space and time coordinates are $x$ (m) and $t$ (s), respectively. The mass transport equations for all species are solved numerically in CHEQMATE by an explicit forward difference method.

The equilibrium part of the CHEQMATE program is essentially the program PHREEQE (Parkhurst et al., 1980). For each chemical element, one aqueous species is selected as the primary species. The rest of the aqueous species are treated as complexes formed by the primary species. For each element, except hydrogen and oxygen, there is a mass conservation equation. The sum of the concentrations of all the species containing that element, plus any dissolution or minus any precipitation from minerals, should equal to the total concentrations of that element originally existing in the system. It is difficult to deal with mass conservation of hydrogen and oxygen in aqueous system. Instead a charge balance and a balance of operational valence are used in PHREEQE. The chemical reactions considered in the program are complex reactions, acid/base neutralisation reactions, redox reactions and mineral dissolution/precipitation reactions. In a recent version of CHEQMATE, sorption reactions can also be modelled.

The system considered is one-dimensional. It is discretised into a number of cells. The left and right cells are boundary cells for mass transport. Different boundary conditions can be modelled, like constant concentration boundary or constant flux boundary. The other cells in between represent the modelled system. Minerals can be allocated in these cells. The pore water are assumed to be in equilibrium with these minerals and concentrations of the aqueous species are determined at certain pH and Eh. A concentration gradient is obtained for an aqueous species when the concentration of that species in different cells is calculated. All the species are then allowed to be transported by diffusion and advection due to the concentration gradient or the groundwater velocity. When new species are transported into a cell, the previous chemical equilibrium condition no longer holds, and all the cells are equilibrated again. By this two-step method (a step of mass transport and a step of chemical equilibrium), spatial and time variations of the contents of minerals and the concentrations of aqueous species can be calculated.

# 4 Model settings

The model used in this study starts from when the bentonite buffer has been saturated with groundwater and all previous transient effects are not considered. Both the oxidation and the low-temperature alteration mechanisms are considered. The ion-exchange and

sorption mechanisms, however, are not considered and will be accounted for in later studies.

The model settings are as follows (Figure 4.1). The thickness of the bentonite buffer in the KBS-3 (1983) concept is about 0.38 m. In the model, a one-dimensional column, 0.38 m long, is selected to represents the bentonite buffer. The column is discretised to 19 cells. The cross-section area of the cells is assumed to be 1.0 $m^2$. Minerals of montmorillonite, calcite and pyrite are assumed to initially exist in each cell. Montmorillonite is the major component of the bentonite. Pyrite is the redox buffer mineral. Calcite is the pH buffer mineral. The quantities of the minerals are chosen from various literature sources. Hematite, pyrite and uraninite are allowed to precipitate during the model simulations. The column is assumed to be a porous medium with a porosity of 30%. As an initial condition the minerals are in equilibrium with the porewater, giving the water certain values of pH, Eh and concentrations of dissolved species.

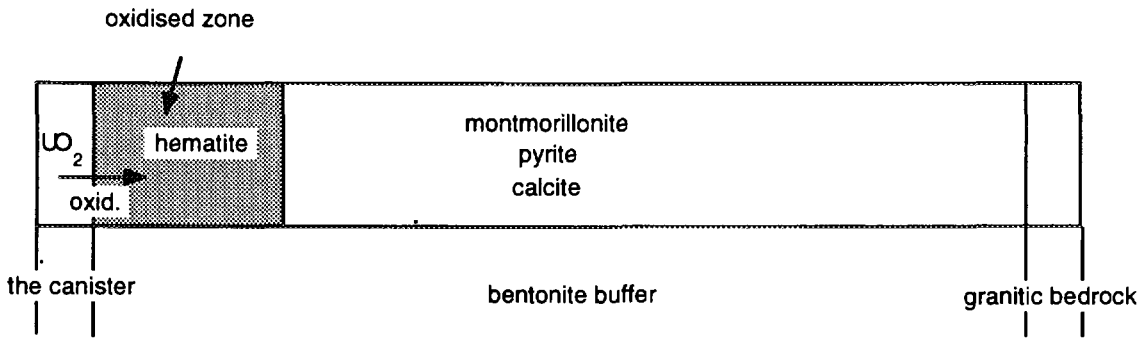


Figure 4.1 Model settings for the study of the stability of the bentonite buffer.

To the left of the column of bentonite buffer, there is one cell to represent the canister. It contains the mineral uraninite. Only the release of uranium is considered in this study. Release of other radionuclides and fission products will be addressed in future studies. Oxidants are assumed to be generated by water radiolysis in the canister, escaped through a small hole (of manufacturing defect) on the canister wall, and transported to the bentonite buffer by diffusion. The oxidants are represented by the equivalent of dissolved oxygen. They are assumed either to oxidise uraninite or to be transported by diffusion to the bentonite column to oxidise pyrite to precipitate hematite. A redox front can propagate through the bentonite buffer to the granitic bedrock when more and more pyrite is oxidised.

To the right of the column, the bentonite is assumed to be in contact with groundwater flowing through some fractures in the granitic bedrock. Another cell is chosen to represent the bedrock. After speciation, the concentrations of the various species in the groundwater in the bedrock are kept constant, based on the argument that the groundwater is constantly refreshed by flows in the fractures. Other boundary conditions can also be assumed in future studies, e.g. a continuous flux boundary, i.e. diffusive flux across the

bentonite-bedrock interface is equal to the advective flow in the fractures of the granitic bedrock.

Only diffusive mass transport is considered in the column that represents the bentonite buffer. This assumption is well-established because the hydraulic conductivity is extremely low in the bentonite buffer. Moreover, the modelled system is assumed to be isothermal, at 25°C.

It should be noted that in this study, the rectangular co-ordinate system is used, because the present version of the CHEQMATE program can handle problems only in this co-ordinate. The simulation results should therefore be understood as related to this co-ordinate, i.e. the radiolytically generated oxidant is released out from a small hole on the canister wall, and the released oxidant oxidises the pyrite in a system that is 0.38 m long with a cross-section area of 1.0 $m^2$.

The model can predict the complicated chemical evolution of the system over time. The time-space variation of the pH, Eh, mineral distribution and detailed speciation of the aqueous phase are the output results of the model. Two consequences are of special interests: the oxidation of pyrite and the alteration of montmorillonite. By analysing the model results, it can provide insight into the two consequences. The long-term properties of the bentonite can be predicted. The validity of the model prediction depends on the conceptual model of the system, and also on the realism of the various input data.

# 5 Input data in the numerical simulations

In this study, 90 aqueous species made up of 12 elements are considered. The twelve elements are Ca, Mg, Na, K, Fe, Al, Si, C, S, U, H and O. Six minerals are included in the simulations. These are calcite, hematite, illite, Na-montmorillonite, pyrite and uraninite. The Na-montmorillonite is the major component of the bentonite buffer. The bentonite buffer also contains small amounts of calcite and pyrite. The uraninite represents the spent fuel. Hematite and illite are not present initially in the system but can precipitate when oxidation and low-temperature alteration of the bentonite buffer take place, respectively.

## 5.1 Initial conditions for the bentonite buffer

Initial conditions for the bentonite buffer include total element concentrations of the dissolved species, as well as an initial guess for the values of pH and Eh of the porewater. The initial amounts of minerals in the bentonite should also be specified. The program then equilibrates the porewater with the existing minerals. The initial guess of pH and Eh values may be changed after the equilibration, and the speciation of all the 90 aqueous species of the 12 elements can be obtained.

There are few data in the literature of the chemistry of the porewater in the bentonite buffer. One set of experimental data on the interaction of bentonite and water (Wanner et al., 1992) were obtained by the reaction of Na-bentonite with both deionised water and Allard's water (Allard et al., 1983). The concentrations of $Na^+$, $Ca^{2+}$, $Mg^{2+}$, $Cl^-$, $SO_4^{-2}$, Alkalinity and pH were given. In our study, the initial input of the total element concentrations of Na, Ca, Mg, S as well as pH are based on the afore-mentioned experimental data. The initial input of total element concentrations of K and Si are taken from another paper in literature (Wanner et al., 1994). The total element concentrations of Fe, Al and C are just assumed to have the same values as in Allard's water (Allard et al., 1983). Initial concentration of uranium in the porewater in the bentonite buffer is assumed to be zero.

The initial input of pH values in the porewater is taken as 9.0, based on the experimental data (Wanner et al., 1992). The initial guess of Eh value is –0.19 V.

The density of the bentonite is taken as 2 000 kg $m^{-3}$ and the porosity 0.30, based on data in the literature (Wanner et al., 1994). The pore diffusivities for all aqueous species in the porewater of the bentonite buffer are assumed to be $5.0 \cdot 10^{-12}$ $m^2$ $s^{-1}$. The effective diffusivity is therefore $1.5 \cdot 10^{-12}$ $m^2$ $s^{-1}$.

In Project-90 (SKI, 1991), the recommended effective diffusivity in bentonite is $4 \cdot 10^{-11}$ $m^2$ $s^{-1}$. Numerical simulations have also been made with this value of effective diffusivity. The results (not presented in this report) do not differ so much from those obtained by assuming a value of $1.5 \cdot 10^{-12}$ $m^2$ $s^{-1}$. The reason is that, within the range of these values of effective diffusivity, mass transport is not the limiting factor for the oxidation of pyrite. The radiolytic oxidant generation is instead the limiting factor. The rate of redox front propagation is thus controlled by the rate of oxidant generation, not by the mass transport of the oxidants in the bentonite buffer.

The amount of montmorillonite initially present in the bentonite is taken as 80% by weight. This gives a value of 14.53 mol $l^{-1}$ of porewater. The amount of calcite in the bentonite is taken as 1.4% by weight (Wanner et al., 1994). The corresponding value is 0.93 mol $l^{-1}$ of porewater. The quantity of the pyrite varies in different sources of the literature. In KBS-3 (1983), the amount is about two hundred milligrams per kilogram of bentonite, which gives a concentration value of $1.1 \cdot 10^{-2}$ mol $l^{-1}$ of porewater. In other sources (e.g. Torstenfelt et al., 1983), the total iron in MX-80 bentonite is given as 2.5 – 3%, of which 25 – 30% is Fe (II). Eriksen and Jacobsson (1983) have also determined the iron content in Na (MX80) bentonite. The Fe(II) content they found was about 1% by weight of bentonite, of which 0.4% is accessible for dissolution and oxidation. The divalent iron exists in bentonite in different forms, like $Fe(OH)_2$ and $FeS_2$. In this model, for the sake of simplicity all the divalent iron is assumed to be in the form of pyrite, another value of the pyrite concentration will be 0.91 mol $l^{-1}$ of porewater.

The initial total element concentrations in the porewater as well as the initial mineral concentrations of the bentonite buffer are shown in Table 5.1.

Table 5.1 Initial values of pH, Eh, total element concentrations in the porewater and the initial mineral concentrations of the bentonite buffer.

| Items | pH, Eh and total element Conc. (mol $l^{-1}$) | Minerals | Mineral conc. (mol $l^{-1}$ of $H_2O$) |
|---|---|---|---|
| pH | 9 | | |
| Eh | –0.19 V | | |
| Ca | $1.00 \cdot 10^{-4}$ | calcite | $9.33 \cdot 10^{-1}$ |
| Mg | $4.00 \cdot 10^{-6}$ | montmorillonite | $1.45 \cdot 10^{1}$ |
| Na | $1.00 \cdot 10^{-1}$ | pyrite | $1.10 \cdot 10^{-2}$ or |
| K | $1.58 \cdot 10^{-5}$ | | $9.10 \cdot 10^{-1}$ |
| Fe | $5.37 \cdot 10^{-5}$ | | |
| Al | $3.71 \cdot 10^{-7}$ | | |
| Si | $1.06 \cdot 10^{-4}$ | | |
| C | $2.02 \cdot 10^{-3}$ | | |
| S | $4.00 \cdot 10^{-2}$ | | |
| U | 0.0 | | |

## 5.2 Boundary condition for the groundwater in the granitic rock

In this study, the composition of the groundwater in the granitic rock is assumed to be the same as Allard's water (Allard et al., 1983). This is the SKB's reference groundwater in the granitic rock. The SKI's reference groundwater, i.e. Andersson's water (Andersson, 1990), is not so different from Allard's water. The total element concentrations used in the simulations are shown in Table 5.2. A constant concentration boundary for the groundwater in the granitic bedrock is assumed. The total element concentrations are speciated by the program to give the concentrations of the 90 aqueous species, at the specified values of pH and Eh. Other types of boundary condition will be explore in future studies, as discussed before.

## 5.3 Boundary condition for the canister

The major component of the spent fuel in the canister is uraninite. After irradiation in the reactor, the fuel pellets are heavily fissured (KBS 3, 1983). In addition, there are gaps between the fuel pellets and the cladding of the fuel rod. Water is distributed in the cracks and gaps. However, little is known about the chemical properties of this water. In this report, the water is assumed to have a pH value of 7.32. Dissolved uranium concentration in the water is assumed to be $5.88 \cdot 10^{-6}$ mol $l^{-1}$. These data are typical values of groundwater in uranium ore bodies. The concentrations of the other elements are all assumed to be zero, because in the present study only the release of uranium is accounted for.

Table 5.2 Boundary condition of the groundwater in the granitic bedrock.

| Items | pH, Eh and Concentrations ($mg\ l^{-1}$) | Concentrations in ($mol\ l^{-1}$) |
|---|---|---|
| pH | 8 | |
| Eh | –0.23 V | |
| Ca | 25 | $6.24 \cdot 10^{-4}$ |
| Mg | 4.3 | $1.77 \cdot 10^{-4}$ |
| Na | 65 | $2.83 \cdot 10^{-3}$ |
| K | 3.9 | $9.97 \cdot 10^{-5}$ |
| Fe | 3.0 | $5.37 \cdot 10^{-5}$ |
| Al | 0.01 | $3.71 \cdot 10^{-7}$ |
| Si | 11 | $5.14 \cdot 10^{-4}$ |
| C | 123 | $2.02 \cdot 10^{-3}$ |
| S | 9.6 | $1.08 \cdot 10^{-4}$ |
| U | 0.0 | 0.0 |

## 5.4 Input data for water radiolysis in the canister

The oxidant production rate by water radiolysis in the canister is taken from the literature (Christensen and Bjergbakke, 1982). The calculations had been carried out from 40 to $10^6$ years on radiolysis from boiling water reactor (BWR) fuel with a burnup of 33 Mwd/t of U, or 2 851 MJ $kg^{-1}$ of U. There were several sets of water radiolysis data corresponding to different conditions. The set used in this study is the one with Fe to catalyse the recombination, i.e. data in Table 8 in Christensen and Bjergbakke (1982).

The original data of the oxidant production rate are fitted to obtain an analytical function of the rate with respect to time (Romero et al., 1995). The data fitting is shown in Figure 5.1. The analytical function of data fitting is also shown in the figure.

The analytical function is adapted in the CHEQMATE program and the oxidants produced in the canister are allowed to be transported into the bentonite buffer. The escape of the oxidants is assumed to be through a small hole on the wall of the canister. This assumption is somehow too conservative, and in future work other assumptions, like oxidant release occurring only after the corrosion penetration of the canister, should be tested.

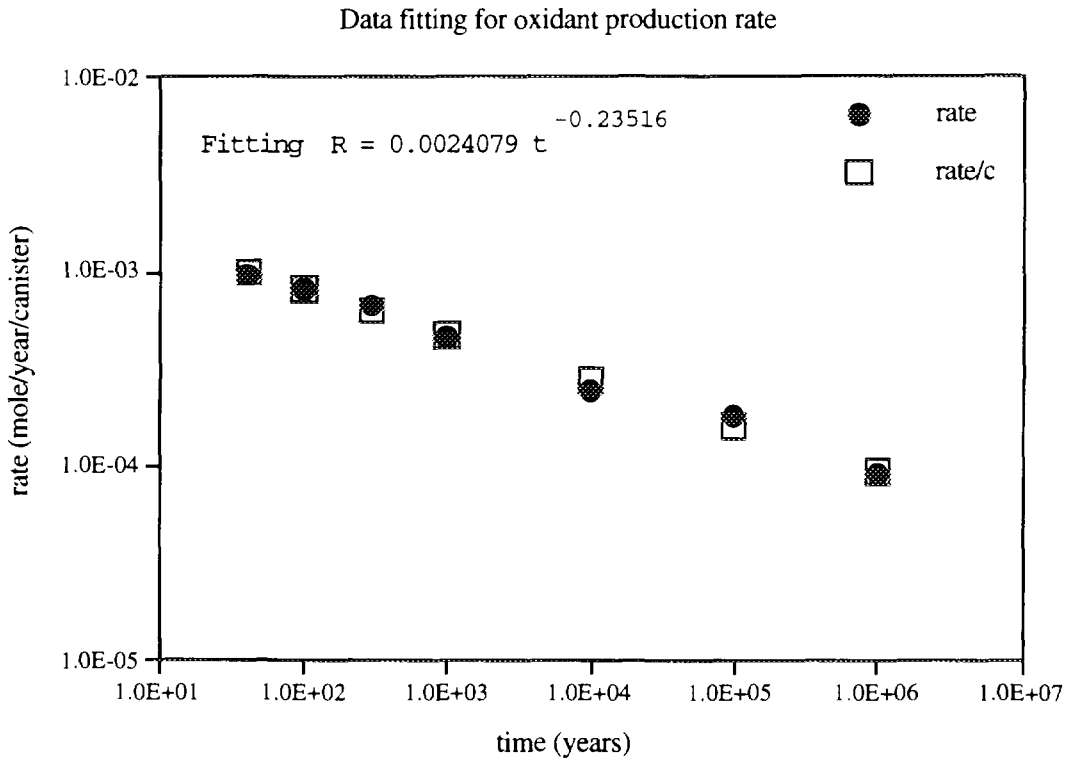


Figure 5.1 Data fitting for the rate of oxidant production by water radiolysis. The solid circles (●) are values from the literature (Christensen and Bjergbakke 1982). The squares (□) are values of data fitting. Both the rate and time co-ordinates are in logarithm scale.

The radiolytically generated oxidant could possibly first oxidise the spent fuel in the canister. Tetra-valent uranium is oxidised to hexa-valent and is released into the bentonite buffer. The hexa-valent uranium, when encountering reducing minerals like pyrite in the bentonite buffer, is reduced again to precipitate as tetra-valent uranium minerals like uraninite. On the other hand, the oxidant could be totally released from the canister into the bentonite buffer, without first oxidising the spent fuel. This point seems to be unreasonable, but with the equilibrium assumption of chemical reactions, and from the mass conservation viewpoint, it does not matter which oxidising species (the oxidants directly produced by water radiolysis or the hexa-valent uranium oxidised by the radiolytically generated oxidants) is introduced into the bentonite buffer. It is however essential for the oxidative dissolution rate of the spent fuel to correctly account for this. The more reasonable situation would be that part of the radiolytically generated oxidant oxidises uraninite in the spent fuel, producing hexa-valent aqueous uranium species which is transported to the bentonite buffer and there it can oxidise the reducing minerals like pyrite. Part of the radiolytically generated oxidant would be directly transported to the bentonite buffer, and oxidises e.g. pyrite there (Neretnieks, 1995).

In this particular study, four cases are considered, based on the assumptions of whether the radiolytically generated oxidant first oxidises uraninite in the spent fuel or not, and

also on the assumption of varying amounts of pyrite initially present in the bentonite buffer.

*Case 1.* The radiolytically generated oxidant all escapes into the bentonite buffer, without first oxidising the spent fuel. The content of pyrite in the bentonite buffer is 200 mg per kg of bentonite.

*Case 2.* The radiolytically generated oxidant all escapes into the bentonite buffer, without first oxidising the spent fuel. The content of pyrite in the bentonite buffer 7.6 g per kg of bentonite.

*Case 3.* The radiolytically generated oxidant first oxidises uraninite in the spent fuel, the produced hexa-valent uranium is then released into the bentonite buffer to oxidise the pyrite. The content of pyrite in the bentonite buffer is 200 mg per kg of bentonite.

*Case 4.* The radiolytically generated oxidant first oxidises uraninite in the spent fuel, the produced hexa-valent uranium is then released into the bentonite buffer to oxidise the pyrite. The content of pyrite in the bentonite buffer is 7.6 g per kg of bentonite.

# 6 Scoping calculations

When mass transport is coupled with geochemical reactions, the evolution of the modelled system becomes very complicated. The full-scale problem must be handled by numerical codes like the CHEQMATE program. Some essential aspects of the system, however, can still be predicted by handy analytical calculations. These simple calculations are essential for successful numerical simulations. On one hand, these scoping calculations can provide insight into the essence of the problems studied, without being entangled in the detailed complexity. On the other hand, these calculations can provide a base-line where the numerical simulation results can be checked and compared with. Examples of the essential aspects of the system are the conservation of mass and the conservation of the redox operational valence (Parkhurst et al., 1980) of the system

In the following, we will give scoping calculations for the conservation of the oxidising equivalents in the system, i.e. the total amount of oxidant introduced into the system should be equal to the amount of the reducing minerals which are oxidised plus any accumulation of the oxidant in the aqueous phase. If the accumulation in the aqueous phase is not significant compared with the amount of the reducing minerals which are oxidised, the oxidant would be practically equal to the reducing minerals which are oxidised.

For Cases 1 and 3, the mineral concentration is 200 mg per kg of bentonite, which is 0.011 mol $l^{-1}$ of porewater. There are altogether 19 cells, with each cell having a cross-section area of 1.0 $m^2$ and a thickness of 0.02 m. The volume of each cell is 0.02 $m^3$. The porosity of the bentonite buffer is assumed to be 0.3. The volume of the porewater in

each cell is thus 0.006 $m^3$ or 6.0 litres. The total amount of the mineral pyrite in the system is 1.254 mol.

One mole of oxygen is 4 equivalents of oxidant. One mole of pyrite is 15 equivalents. It consumes 3.75 moles of oxygen to oxidise one mole of pyrite. To oxidise 1.254 moles of pyrite totally in the system, it needs 4.7025 moles of oxygen.

The production rate of oxidant (oxygen) is

$$r(t) = 0.0024079t^{-0.23516} \tag{6.1}$$

where $r$ is the production rate in mol $yr^{-1}$ per canister and $t$ is time in years. The cumulative amount of oxidant produced in $t$ years is

$$acc = \int_0^t r(\tau)d\tau = 0.00314824\ t^{0.76484} \tag{6.2}$$

When the pyrite concentration in the bentonite is 200 mg $kg^{-1}$ of porewater, the time for all of the pyrite in the system to be oxidised is obtained from the following equation:

$$0.00314824\ t^{0.76484} = 4.7025 \tag{6.3}$$

The time is $1.4 \cdot 10^4$ years. This means that the redox front breaks through the bentonite buffer in about 14 000 years.

When the concentration of pyrite in the bentonite buffer is 0.91 mol $l^{-1}$ of porewater, i.e. slightly less than 1% by weight of pyrite, the redox front will not break through the bentonite buffer up to $1.0 \cdot 10^6$ years, by which time 122 mol of oxygen has been produced. It can be calculated, using a similar procedure as before, that the redox front will reach a distance 0.12 m from the canister inside the bentonite buffer.

The scoping calculations can not provide the detailed perspective of the geochemical evolution of the modelled system. Numerical simulations are needed. The numerical simulation results with the CHEQMATE program will be present in the following section.

# 7 Simulation results

The output of the CHEQMATE program includes spatial-time variations of all the aqueous species and minerals included in the model. In principle the concentrations of all the aqueous species and minerals at every time step can be obtained. In reality only concentrations of certain aqueous species and minerals of special interest are required to be output at certain time steps.

The simulation results of the four cases are presented below. Results of some cases are presented in detail. Results of other cases will be present only in brief.

## 7.1 Modelling results of Case 1

In this case, it is assumed that the radiolytically generated oxidant does not oxidise the spent fuel in the canister and the amount of pyrite in the bentonite is 200 mg per kg of bentonite.

The pH and Eh profiles in the bentonite buffer 7000 years after the sealing of the repository are presented in Figures 7.1.1 and 7.1.2. The horizontal axis is the distance in metres from the canister wall. To the left of the one-dimensional column of the bentonite buffer is the canister and to the right is the granitic bedrock. Consequently the two end-points on the left and right sides of the curves in the figures represent the conditions in the canister and the granitic bedrock, respectively.

The contents of hematite and pyrite in the bentonite buffer 7000 years after the sealing of the repository are shown in Figure 7.1.3. The mineral contents of Na-montmorillonite and illite are shown in Figure 7.1.4. In Figures 7.1.5 to 7.1.8, the total element concentration profiles of Ca, Mg, Na, K, Al, Si, C, S, Fe in the aqueous phase as well as the concentration profile of dissolved oxygen are shown respectively.

The results clear show that the pyrite in the bentonite buffer can be oxidised to hematite. The redox front has propagated to a place between 0.20 to 0.22 m from the canister after 7000 years. The results also show that the break-through time of the redox front (the redox front has propagated through the bentonite buffer and reached the granitic bedrock) is between $1.4 \cdot 10^4$ to $1.45 \cdot 10^4$ years. This is in agreement with the result of scoping calculations in Section 6.

In Figure 7.1.4, the content of illite is zero. The low-temperature alteration of Na montmorillonite to illite has not occurred. The conclusion is that, under the geochemical conditions of this study, Na montmorillonite is more stable than illite and conversion to illite will not occur. The loss of swelling ability and the increase of hydraulic conductivity due to the conversion of montmorillonite to illite is unlikely to happen.

The pH values in the bentonite buffer shown in Figure 7.1.1 are between 7.4 and 8.1. There is a gradient of the pH values pointing from the granitic bedrock into the bentonite buffer. The gradient of the proton ($H^+$) is just the opposite. The proton is continuously released out from the bentonite buffer to the granitic bedrock. The initial pH value in the bentonite in the simulation is 9. When pyrite is oxidised to hematite, proton is released. This is the reason for the low pH shown in the simulation result after pyrite has been oxidised. The Eh profile in Figure 7.1.2 indicates that in the oxidised zone in the bentonite buffer, the Eh values could be as high as 0.79 V. In the reducing zone, the Eh values are between -0.20 and –0.25 V. The sharp redox front is clearly shown in the figure.

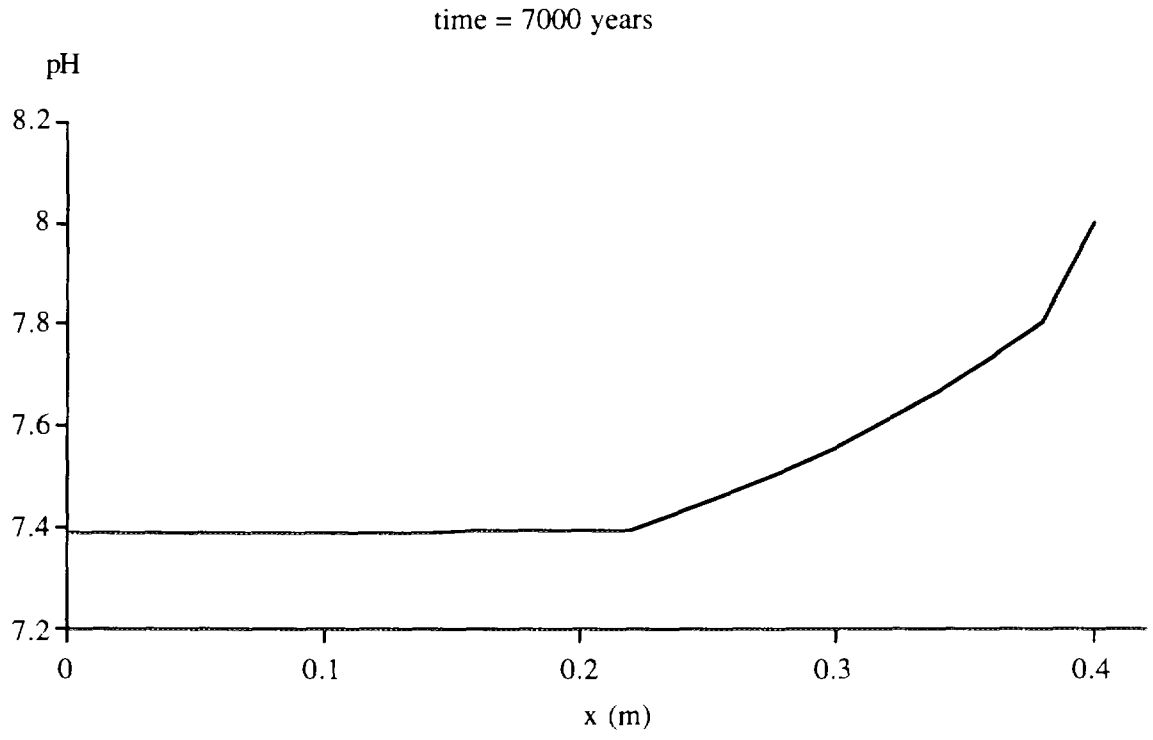


Figure 7.1.1 pH profile in the bentonite buffer 7000 years after the sealing of the repository.

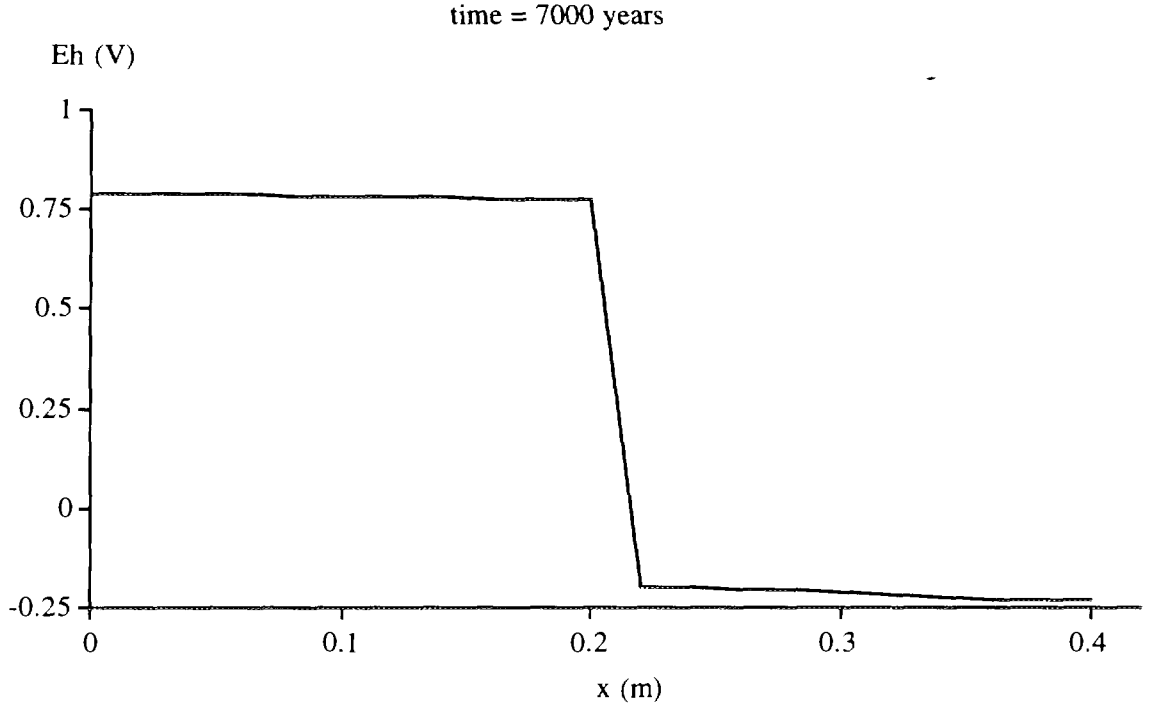


Figure 7.1.2 Eh (V) profile in the bentonite buffer 7000 years after the sealing of the repository.

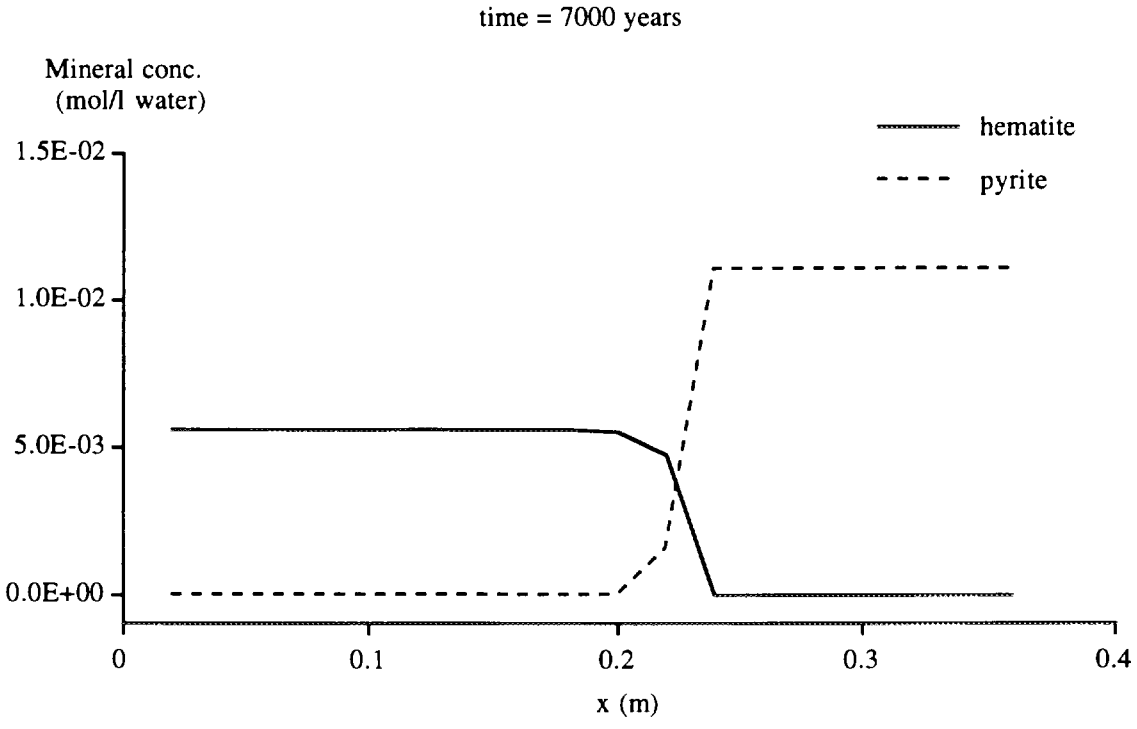


Figure 7.1.3 Contents of hematite and pyrite in the bentonite buffer 7000 years after the sealing of the repository. The vertical axis is in mol $l^{-1}$ of porewater.

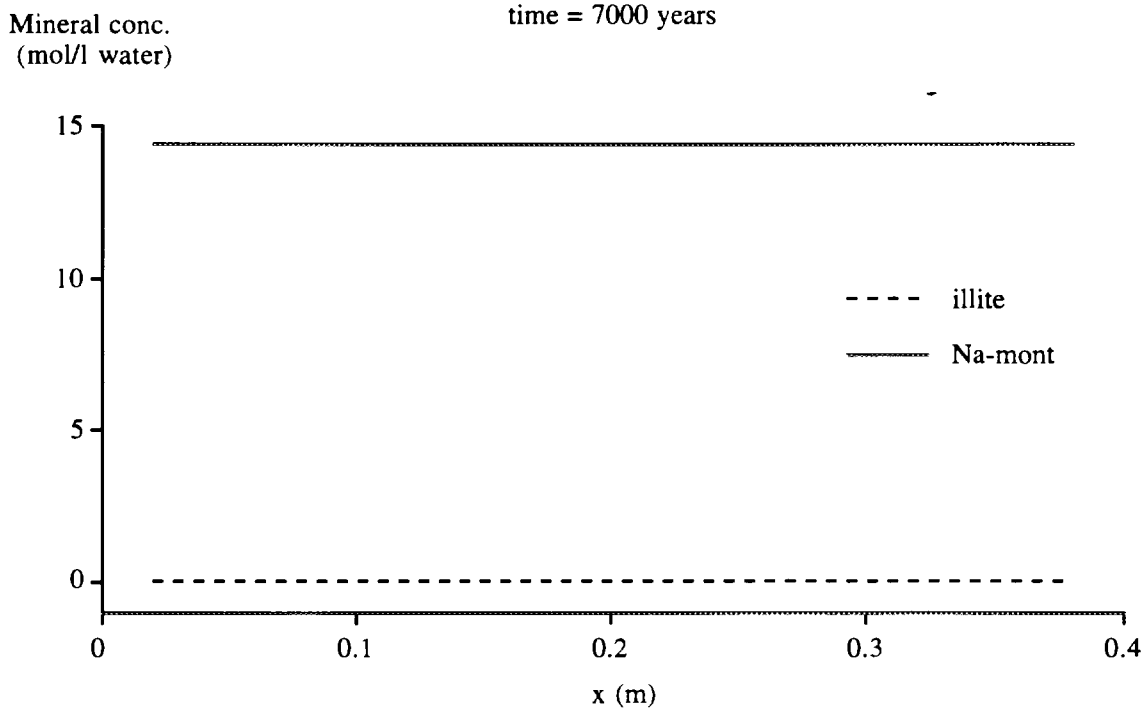


Figure 7.1.4 Contents of Na-montmorillonite and illite in the bentonite buffer 7000 years after the sealing of the repository. The vertical axis is in mol $l^{-1}$ of porewater. The content of illite is zero.

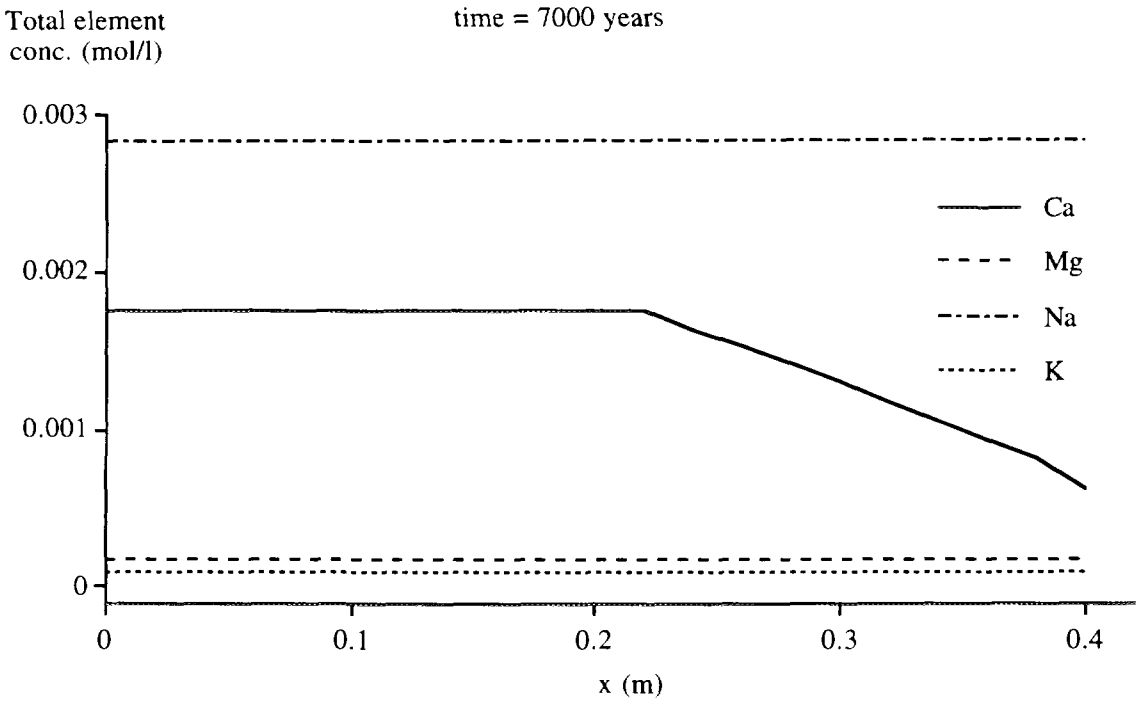


Figure 7.1.5 Total element concentrations of Ca, Mg, Na and K in the porewater of the bentonite buffer 7000 years after the sealing of the repository.

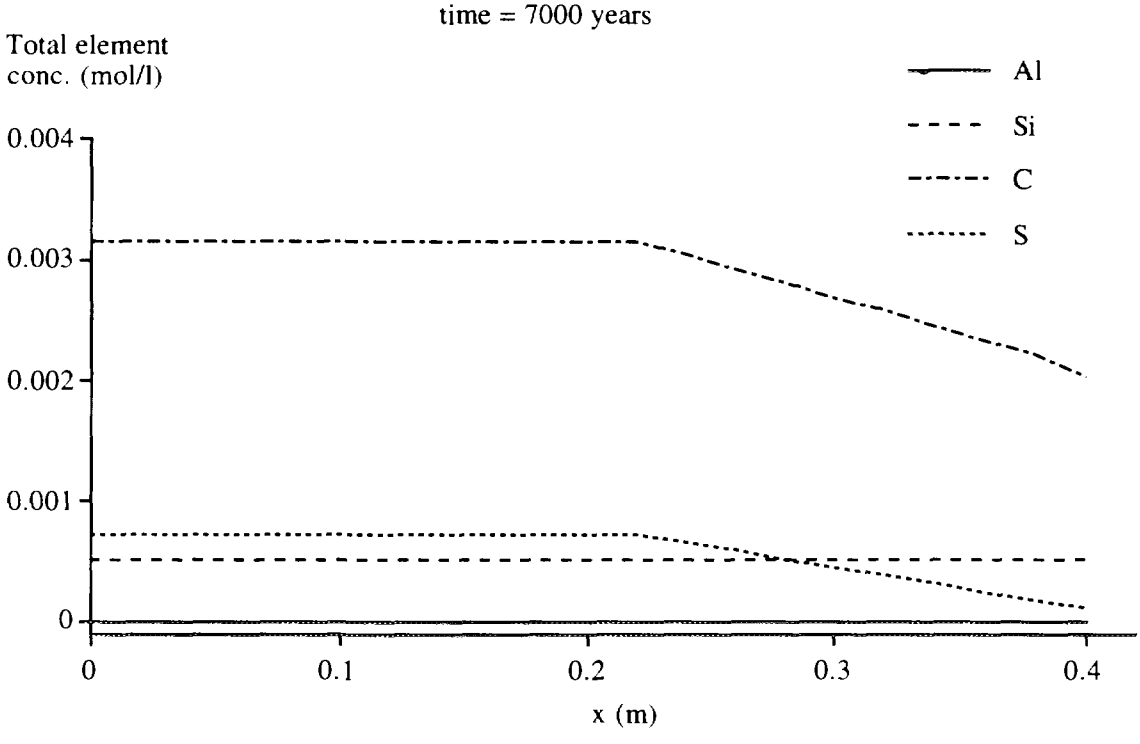


Figure 7.1.6 Total element concentrations of Al, Si, C and S in the porewater of the bentonite buffer 7000 years after the sealing of the repository.

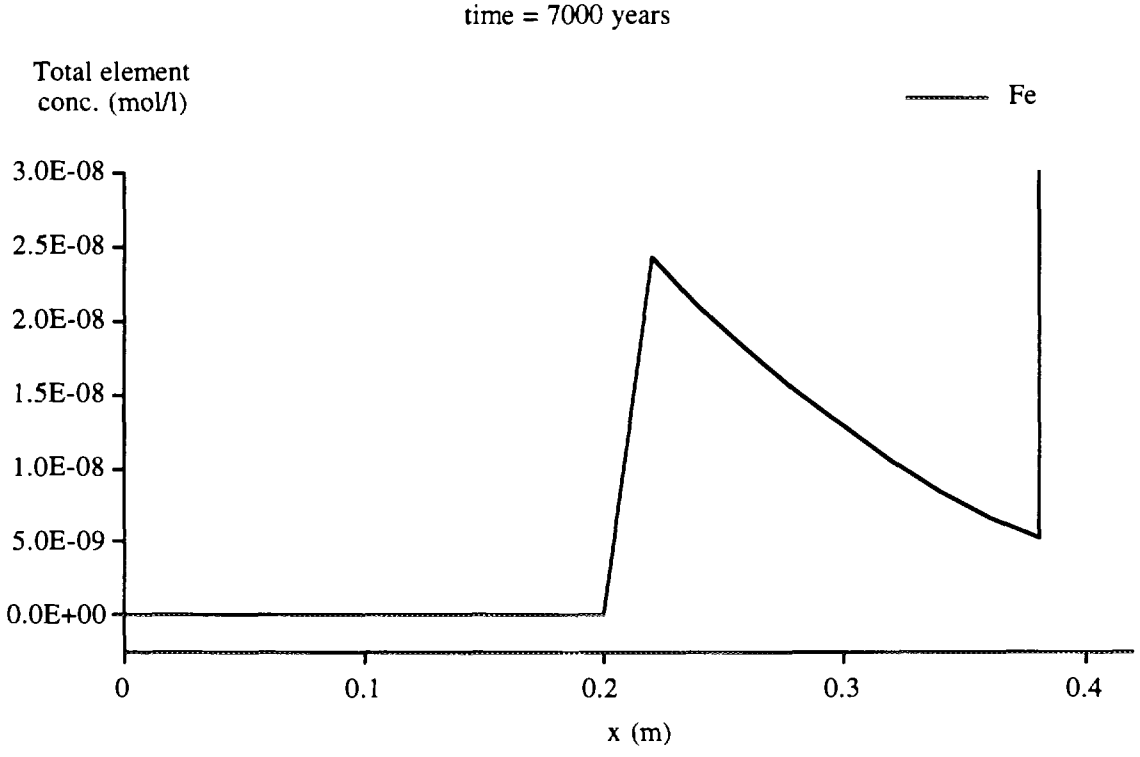


Figure 7.1.7 Total element concentrations of Fe in the porewater of the bentonite buffer 7000 years after the sealing of the repository.

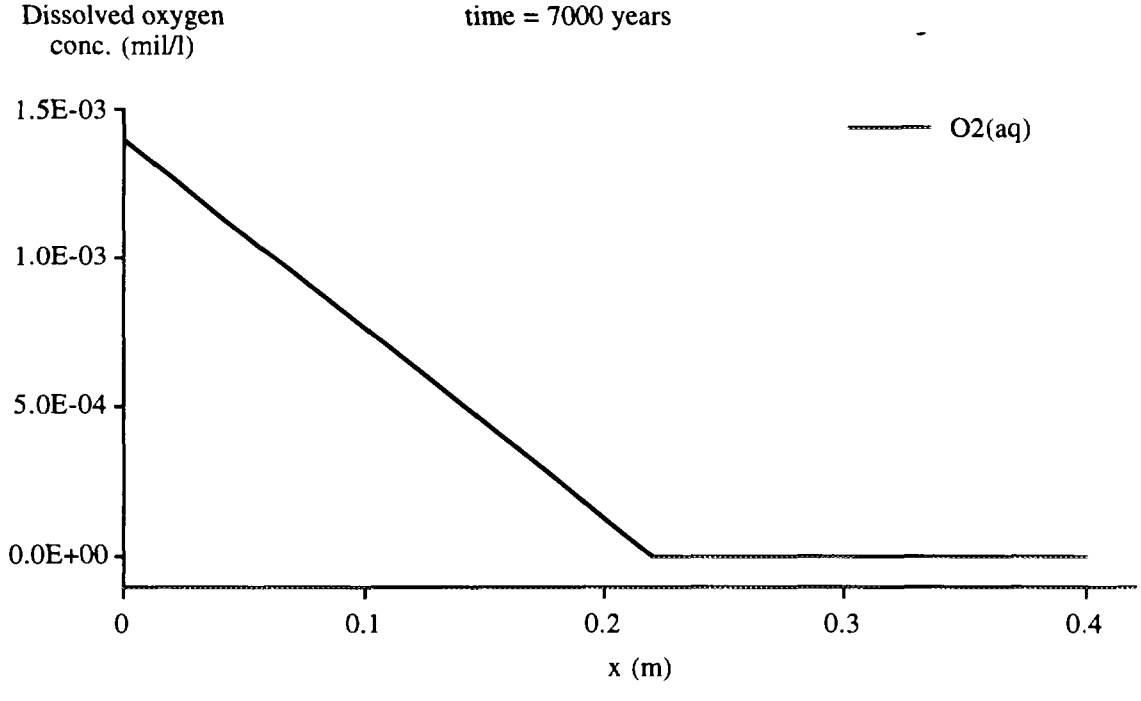


Figure 7.1.8 Dissolved oxygen concentration in the porewater of the bentonite buffer 7000 years after the sealing of the repository.

The profiles of the total element concentrations are shown in Figures 7.1.5 to 7.1.7. From the profiles the concentration gradient and therefore the direction of the diffusive mass transport can clearly be seen. For example, at this time, the profiles of Mg, Na, K, Si and Al have been more or less evened out. There is, however, release of Ca, C and S from the bentonite buffer to the granitic bedrock. The profiles of those elements that are released out are more or less straight lines, which indicates that a pseudo steady-state has been achieved at this time. The reason for that montmorillonite has not been altered to illite can also partly be explained from the concentration gradients of K, Al and Si. For the alteration to occur, potassium has to be transported into the bentonite, silicon must be transported out. Aluminium is needed to substitute silicon in the tetrahedral sites. The aluminium can either be transported from the granitic rock into the bentonite or it can be the aluminium in the octahedral sites already in the montmorillonite crystal structure. At the time 7000 years, there is no concentration gradient for the species made up of these element. At earlier times (not shown in the figures), K and Al are indeed introduced into the bentonite buffer by diffusion, but the concentration gradient of total silicon points from the granitic bedrock toward the bentonite, which means that the silicon is not transported out of the bentonite. Without the release of silicon to the outside of the bentonite buffer, the montmorillonite is stable. Of course the concentration gradients are just the reflection of chemical equilibrium of the system. The stability of Na-montmorillonite actually is due to the chemical stability of the mineral in the pH, Eh ranges of the system.

It should be noted that the chemical stability of smectite depends upon the choice of the models of bentonite-water interaction. A stoichiometric mineral of montmorillonite is assumed in the present model. The results discussed above indicate that the montmorillonite is chemically stable with respect to stoichiometric minerals of hydrous mica (illite in this case). When other models are used, e.g. the solid-solution model, one type of montmorillonite solid-solution may be non-stable with respect to other types of solid-solutions with different end-member components (Arthur and Apted, 1994).

Simulation results of other time steps are also obtained. The total simulation time corresponds to about $1.6 \cdot 10^4$ years, somewhat longer than the break-through time. Results in other times show that the pH values in the bentonite buffer are between 7.1 to 7.8 in the bentonite. In the oxidised zone the Eh values vary between 0.75 to 0.78 V.

Figure 7.1.7 shows the concentration profile of total iron in the aqueous phase at 7000 years. The speciation (not shown in the results) indicates that the iron is predominantly in the di-valent state. The concentration of Fe(II) in the bedrock is out of the plot range of the figure, which is always much larger than that in the bentonite buffer. Consequently Fe(II) is continuously transported into the bentonite. When the Fe(II) meets the $SO_4^{-2}$ released out from the bentonite (the $SO_4^{-2}$ is a product of pyrite oxidation), part of the Fe(II) is oxidised to hematite and precipitates at the interface of the bentonite buffer and the granitic bedrock. Some of the $SO_4^{-2}$ is reduced to sulphide at the interface, and reacts with the rest of the Fe(II) to precipitate as pyrite. This phenomenon has also been predicted in the natural analogue studies of the Cigar Lake uranium deposit (Liu, 1995).

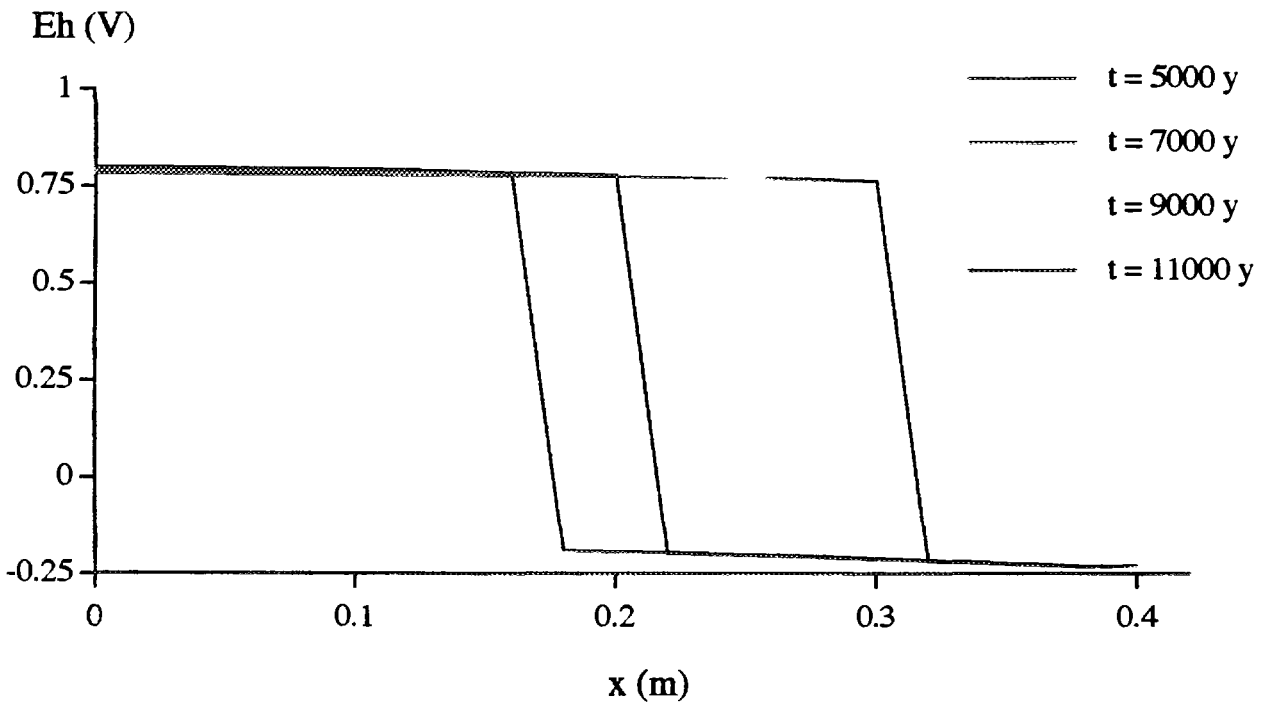


Figure 7.1.9 Changes of Eh (V) profiles in the bentonite buffer with time.

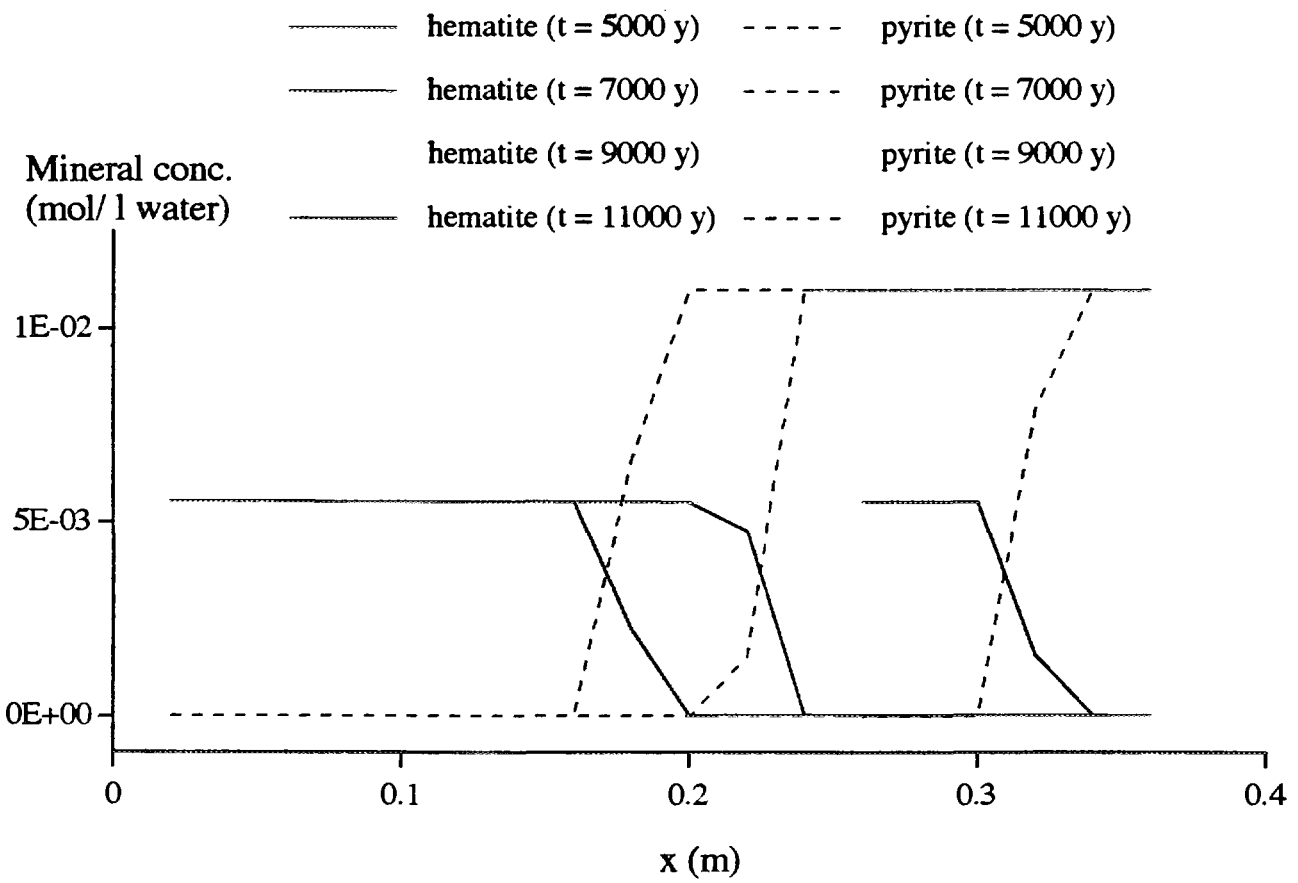


Figure 7.1.10 Changes of the contents of hematite and pyrite in the bentonite buffer with time.

The concentration profile of dissolved oxygen at 7000 years is shown in Figure 7.1.8. The gradient at the oxidised zone is constant, which also indicates that a pseudo steady state has been reached. In the reducing zone, the oxygen concentration is virtually zero.

The variation of the Eh profiles and the contents of hematite and pyrite in the bentonite buffer are shown in Figures 7.1.9 and 7.1.10. The propagation of the redox front with time is well demonstrated in these two figures.

## 7.2 Modelling results of Case 2

In Case 2, it is still assumed that all the oxidant generated by water radiolysis is transported into the bentonite buffer, without first oxidising the uraninite in the spent fuel. It differs from Case 1 in that the initial content of the mineral pyrite in the bentonite is assumed to be 0.76%, 38 times larger than that in Case 1.

The results will not be presented in detail. The redox front propagates only 0.1 m from the canister in the bentonite buffer $1.0 \cdot 10^6$ years after the sealing of the repository. This result is expected as the initial content of the reducing mineral pyrite is much larger in Case 2 than in Case 1. The result implies that less than 1 percent of pyrite in the bentonite can ensure a reducing environment in the near field of the repository up to 1 million years. The radiolytic oxidant production rate decreases very rapidly with time. The reducing environment in the near field can thus prevail even for a much longer time than 1 million years.

In this case, the simulation results still indicate that the Na-montmorillonite has not been converted to illite up to $1.0 \cdot 10^6$ years. This implies that montmorillonite in the bentonite buffer in chemically stable under the conditions that can possibly prevail in the near field of the repository.

It is assumed that in the bentonite there is an initial concentration of calcite of 1.4% by weight. This calcite functions as pH buffer. In Case 2, some of the calcite near the canister as well as close to the granitic bedrock has been dissolved. In Case 1, however, the simulation results show that calcite has not been dissolved. The reason for this is that, in Case 2, there is relatively a larger amount of pyrite. When the pyrite is oxidised, more acidity is produced in Case 2 than in Case 1. In Case 2, the pH values are somehow lower where calcite has been dissolved, compared with the results of Case 1. The low pH values are in the range of 6.5 to 7.7.

## 7.3 Modelling results of Case 3

In this case, the radiolytically generated oxidant is assumed to first oxidise uraninite in the spent fuel, the produced hexa-valent uranium is then released into the bentonite buffer to

oxidise the pyrite. The content of pyrite in the bentonite buffer is 200 mg per kg of bentonite.

The simulation results show that the redox front propagates at the same rate as in Case 1, in which the same initial amount of pyrite is assumed. This is expected. From the viewpoint of mass conservation, the front should propagate at the same rate, when the rate of oxidant production is the same, and there is the same amount of pyrite in the bentonite.

The model results indicate that, even the rate of redox front propagation is the same, the chemical properties are different in Cases 1 and 3. This is illustrated by Table 7.3.1 and 7.3.2. The two tables show the equilibrium speciation of the aqueous phase in the cells close to the canister. Table 7.3.1 is the speciation for Case 1 and Table 7.3.2 is the speciation for Case 3. The time is about 10 000 years after the sealing of the repository.

In Table 7.3.1 the dominant oxidising species is the dissolved oxygen (No. 22 in the list). The concentration of it is about $1.58 \cdot 10^{-3}$ mol $l^{-1}$. In Table 7.3.2 the dominant oxidising species are some U(VI), their total concentrations are about $1.38 \cdot 10^{-3}$ mol $l^{-1}$.

Table 7.3.1 Equilibrium speciation of the dominating species in aqueous phase in Cell 2 for Case 1. The time is about 10 000 years.

CELL NO 2 TIME STEP 10000

TOTAL MOLALITIES OF ELEMENTS

| ELEMENT | MOLALITY | LOG MOLALITY |
|---|---|---|
| CA | 1.303910D-03 | -2.8848 |
| MG | 1.768091D-04 | -3.7525 |
| NA | 2.827247D-03 | -2.5486 |
| K | 9.974930D-05 | -4.0011 |
| FE | 9.847057D-16 | -15.0067 |
| AL | 1.642417D-09 | -8.7845 |
| SI | 5.131162D-04 | -3.2898 |
| C | 2.696028D-03 | -2.5693 |
| S | 4.515656D-04 | -3.3453 |
| U | 2.555325D-06 | -5.5926 |

----DESCRIPTION OF SOLUTION----

| | |
|---|---|
| PH = | 7.5557 |
| PE = | 13.2641 |
| EH = | 0.7847 |
| ACTIVITY H2O = | 0.9998 |
| IONIC STRENGTH = | 0.0063 |
| TEMPERATURE = | 25.0000 |
| ELECTRICAL BALANCE = | 2.4180D-03 |
| THOR = | 1.9823D-02 |
| ITERATIONS = | 21 |

DISTRIBUTION OF SPECIES

| I | SPECIES | Z | MOLALITY | LOG MOLAL | ACTIVITY | LOG ACT | GAMMA | LOG GAM |
|---|---|---|---|---|---|---|---|---|
| 1 | H+ | 1.0 | 3.027E-08 | -7.519 | 2.782E-08 | -7.556 | 9.191E-01 | -0.037 |
| 2 | E- | -1.0 | 5.444E-14 | -13.264 | 5.444E-14 | -13.264 | 1.000E+00 | 0.000 |
| 4 | CA+2 | 2.0 | 1.226E-03 | -2.911 | 8.749E-04 | -3.058 | 7.135E-01 | -0.147 |
| 5 | MG+2 | 2.0 | 1.669E-04 | -3.777 | 1.191E-04 | -3.924 | 7.135E-01 | -0.147 |
| 6 | NA+ | 1.0 | 2.820E-03 | -2.550 | 2.592E-03 | -2.586 | 9.191E-01 | -0.037 |
| 7 | K+ | 1.0 | 9.955E-05 | -4.002 | 9.149E-05 | -4.039 | 9.191E-01 | -0.037 |
| 10 | H4SIO4 | 0.0 | 5.108E-04 | -3.292 | 5.115E-04 | -3.291 | 1.001E+00 | 0.001 |
| 12 | SO4-2 | -2.0 | 3.917E-04 | -3.407 | 2.794E-04 | -3.554 | 7.135E-01 | -0.147 |
| 21 | OH- | -1.0 | 3.911E-07 | -6.408 | 3.594E-07 | -6.444 | 9.191E-01 | -0.037 |
| 22 | O2(AQ) | 0.0 | 1.579E-03 | -2.802 | 1.581E-03 | -2.801 | 1.001E+00 | 0.001 |
| 24 | HCO3- | -1.0 | 2.506E-03 | -2.601 | 2.303E-03 | -2.638 | 9.191E-01 | -0.037 |
| 26 | H2CO3 | 0.0 | 1.432E-04 | -3.844 | 1.434E-04 | -3.843 | 1.001E+00 | 0.001 |
| 52 | FE(OH)2+ | 1.0 | 6.397E-16 | -15.194 | 5.879E-16 | -15.231 | 9.191E-01 | -0.037 |
| 53 | FE(OH)3 | 0.0 | 2.479E-16 | -15.606 | 2.483E-16 | -15.605 | 1.001E+00 | 0.001 |
| 54 | FE(OH)4- | -1.0 | 9.708E-17 | -16.013 | 8.923E-17 | -16.050 | 9.191E-01 | -0.037 |
| 61 | AL(OH)3 | 0.0 | 3.324E-10 | -9.478 | 3.329E-10 | -9.478 | 1.001E+00 | 0.001 |
| 62 | AL(OH)4- | -1.0 | 1.302E-09 | -8.885 | 1.197E-09 | -8.922 | 9.191E-01 | -0.037 |
| 87 | ULCO32-2 | -2.0 | 1.622E-06 | -5.790 | 1.157E-06 | -5.937 | 7.135E-01 | -0.147 |
| 88 | ULCO33-4 | -4.0 | 9.077E-07 | -6.042 | 2.352E-07 | -6.629 | 2.591E-01 | -0.586 |

---- LOOK MIN IAP ----

| PHASE | LOG IAP | LOG KT | LOG IAP/KT |
|---|---|---|---|
| CALCITE | -8.4700 | -8.4700 | 0.0000 |
| HEMATITE | 22.0500 | 22.0500 | 0.0000 |
| ILLITE | 8.3900 | 9.8000 | -1.4100 |
| MONT-NA | 3.0600 | 3.0600 | 0.0000 |
| PYRITE | -338.6014 | -85.7800 | -252.8214 |
| URANINIT | -29.2208 | -4.6000 | -24.6208 |

Table 7.3.2 Equilibrium speciation of the dominating species in aqueous phase in Cell 2 for Case 3. The time is about 10 000 years.

CELL NO 2 TIME STEP 10000

TOTAL MOLALITIES OF ELEMENTS

| ELEMENT | MOLALITY | LOG MOLALITY |
|---|---|---|
| CA | 1.366945D-03 | -2.8642 |
| MG | 1.768092D-04 | -3.7525 |
| NA | 2.827247D-03 | -2.5486 |
| K | 9.974930D-05 | -4.0011 |
| FE | 2.089587D-15 | -14.6799 |
| AL | 2.225885D-09 | -8.6525 |
| SI | 5.131176D-04 | -3.2898 |
| C | 2.759063D-03 | -2.5592 |

| | | |
|---|---|---|
| S | 4.728010D-04 | -3.3253 |
| U | 3.080498D-03 | -2.5114 |

----DESCRIPTION OF SOLUTION----

| | |
|---|---|
| PH = | 7.9819 |
| PE = | 2.1514 |
| EH = | 0.1273 |
| ACTIVITY H2O = | 0.9999 |
| IONIC STRENGTH = | 0.0093 |
| TEMPERATURE = | 25.0000 |
| ELECTRICAL BALANCE = | 2.4180D-03 |
| THOR = | 3.2356D-02 |
| ITERATIONS = | 27 |

DISTRIBUTION OF SPECIES

| I | SPECIES | Z | MOLALITY | LOG MOLAL | ACTIVITY | LOG ACT | GAMMA | LOG GAM |
|---|---|---|---|---|---|---|---|---|
| 1 | H+ | 1.0 | 1.152E-08 | -7.938 | 1.043E-08 | -7.982 | 9.046E-01 | -0.044 |
| 2 | E- | -1.0 | 7.057E-03 | -2.151 | 7.057E-03 | -2.151 | 1.000E+00 | 0.000 |
| 4 | CA+2 | 2.0 | 1.304E-03 | -2.885 | 8.733E-04 | -3.059 | 6.696E-01 | -0.174 |
| 5 | MG+2 | 2.0 | 1.695E-04 | -3.771 | 1.135E-04 | -3.945 | 6.696E-01 | -0.174 |
| 6 | NA+ | 1.0 | 2.822E-03 | -2.549 | 2.553E-03 | -2.593 | 9.046E-01 | -0.044 |
| 7 | K+ | 1.0 | 9.955E-05 | -4.002 | 9.006E-05 | -4.045 | 9.046E-01 | -0.044 |
| 8 | FE+2 | 2.0 | 1.265E-15 | -14.898 | 8.471E-16 | -15.072 | 6.696E-01 | -0.174 |
| 10 | H4SIO4 | 0.0 | 5.067E-04 | -3.295 | 5.078E-04 | -3.294 | 1.002E+00 | 0.001 |
| 12 | SO4-2 | -2.0 | 4.138E-04 | -3.383 | 2.771E-04 | -3.557 | 6.696E-01 | -0.174 |
| 21 | OH- | -1.0 | 1.060E-06 | -5.975 | 9.591E-07 | -6.018 | 9.046E-01 | -0.044 |
| 24 | HCO3- | -1.0 | 9.560E-04 | -3.020 | 8.648E-04 | -3.063 | 9.046E-01 | -0.044 |
| 34 | CASO4 | 0.0 | 4.930E-05 | -4.307 | 4.941E-05 | -4.306 | 1.002E+00 | 0.001 |
| 52 | FE(OH)2+ | 1.0 | 2.436E-16 | -15.613 | 2.203E-16 | -15.657 | 9.046E-01 | -0.044 |
| 53 | FE(OH)3 | 0.0 | 2.477E-16 | -15.606 | 2.483E-16 | -15.605 | 1.002E+00 | 0.001 |
| 54 | FE(OH)4- | -1.0 | 2.632E-16 | -15.580 | 2.381E-16 | -15.623 | 9.046E-01 | -0.044 |
| 61 | AL(OH)3 | 0.0 | 1.913E-10 | -9.718 | 1.917E-10 | -9.717 | 1.002E+00 | 0.001 |
| 62 | AL(OH)4- | -1.0 | 2.033E-09 | -8.692 | 1.839E-09 | -8.735 | 9.046E-01 | -0.044 |
| 82 | UL4(OH)7 | 1.0 | 3.612E-04 | -3.442 | 3.267E-04 | -3.486 | 9.046E-01 | -0.044 |
| 84 | UL3(OH)5 | 1.0 | 1.664E-04 | -3.779 | 1.505E-04 | -3.822 | 9.046E-01 | -0.044 |
| 87 | ULCO32-2 | -2.0 | 4.311E-04 | -3.365 | 2.887E-04 | -3.540 | 6.696E-01 | -0.174 |
| 88 | ULCO33-4 | -4.0 | 2.924E-04 | -3.534 | 5.879E-05 | -4.231 | 2.011E-01 | -0.697 |
| 95 | UL3(OH)7 | -1.0 | 1.303E-04 | -3.885 | 1.179E-04 | -3.929 | 9.046E-01 | -0.044 |

---- LOOK MIN IAP ----

| PHASE | LOG IAP | LOG KT | LOG IAP/KT |
|---|---|---|---|
| CALCITE | -8.4700 | -8.4700 | 0.0000 |
| HEMATITE | 22.0500 | 22.0500 | 0.0000 |
| ILLITE | 8.2873 | 9.8000 | -1.5127 |
| MONT-NA | 3.0600 | 3.0600 | 0.0000 |
| PYRITE | -180.0170 | -85.7800 | -94.2370 |
| URANINIT | -4.6000 | -4.6000 | 0.0000 |

The simulation results of Case 3 also show that, the uraninite that has been oxidised in the spent fuel re-precipitates in the bentonite buffer where hematite precipitates. As long as the pyrite in the bentonite has not been depleted, the release of uranium to the granitic rock is very small, on the order of $10^{-11}$ mol $m^{-2}$ $a^{-1}$. After the break-through of the redox front, the release rate of uranium could be as high as $10^{-4}$ mol $m^{-2}$ $a^{-1}$.

The pH values are between 7.1 and 8.2. The Eh values in the oxidised zone in the bentonite buffer are between 0.113 to 0.157 V, which is much less than those of Case 1 (around 0.79 V). The reason for the low values of Eh is that where the pyrite has been oxidised, uraninite precipitates. In the reducing zone, the Eh values are about the same as those in the reducing zone of Case 1.

In Case 3, the results show that there is still no low-temperature alteration of Na-montmorillonite to illite.

## 7.4 Modelling results of Case 4

The chemical aspects of the modelling results of Case 4 are similar to those of Case 3. The propagation rate of the redox front is that same as in Case 2, since there is the same amount of pyrite in the bentonite buffer in both cases.

In Figure 7.4.1 the Eh profiles in the bentonite at the time $1.0 \cdot 10^6$ years is shown. The Eh value in the oxidised zone is about 0.2 V, in the reducing zone it ranges from –0.25 to –0.15 V.

In Figure 7.4.2 the total element concentration of uranium in the aqueous phase in the bentonite is shown. When pyrite in the bentonite has not been completely depleted, the concentration gradient of dissolved uranium at the interface between the bentonite buffer and the granitic rock is small and the release of uranium to the bedrock is consequently small. The concentration gradient in the oxidised zone is a straight line, which means that the steady state has been achieved.

In Figure 7.4.3 the concentration profiles of pyrite and hematite are shown. The redox front is clearly seen in the bentonite buffer.

In Figure 7.4.4 the concentration profile of uraninite is shown. It demonstrates clearly that uraninite precipitates in the oxidised zone after the redox front has passed through. The amount of uraninite precipitated is about 6.8 mol $l^{-1}$ of porewater, which can account roughly 28% by weight of the bentonite buffer if the density is still assumed to be 2000 kg $m^{-3}$. The uraninite has to precipitate in the porewater. The amount of precipitation is about 1 800 kg per cubic metre of porewater. As the density of uraninite is larger than this figure, the pore has not been plugged by the precipitation of uraninite in this case.

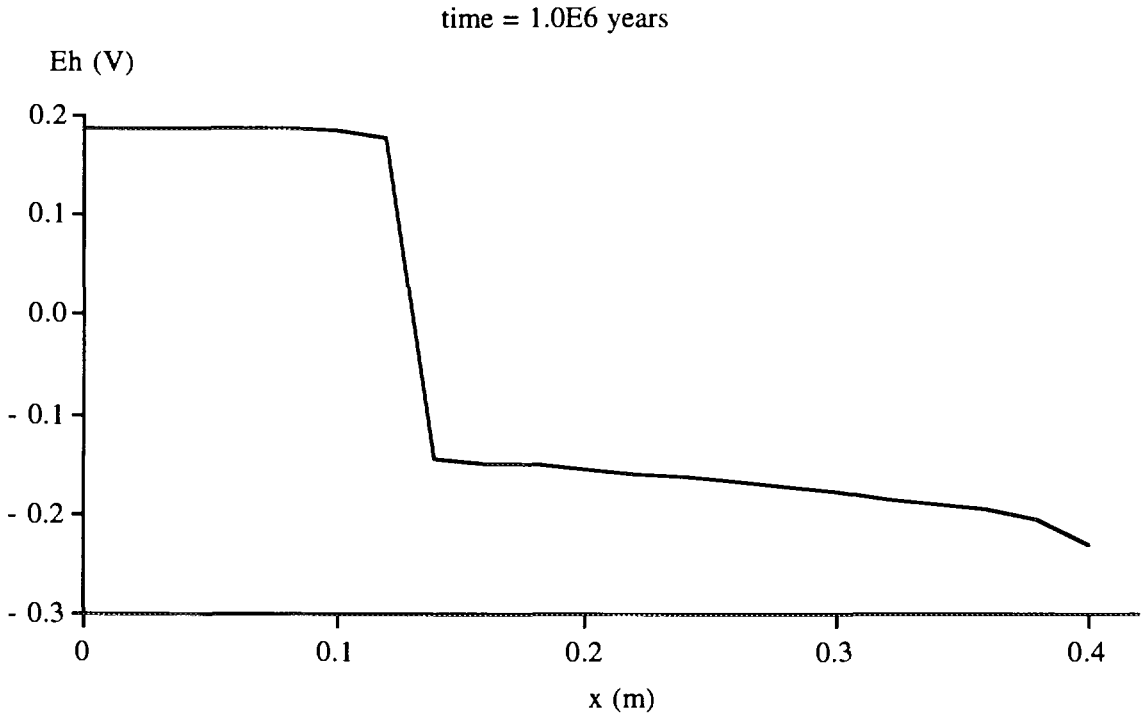


Figure 7.4.1 Eh profiles in the bentonite buffer $1.0 \cdot 10^6$ years after the sealing of the repository.

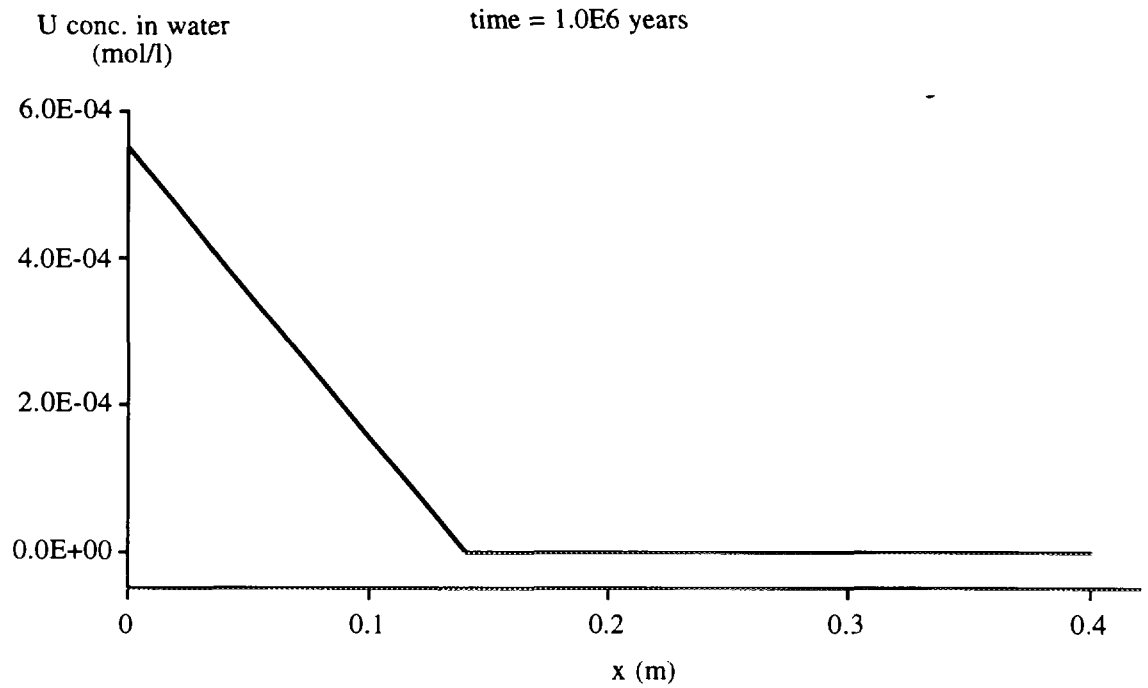


Figure 7.4.2 Profile of the total element concentration of uranium in the porewater in the bentonite buffer $1.0 \cdot 10^6$ years after the sealing of the repository.

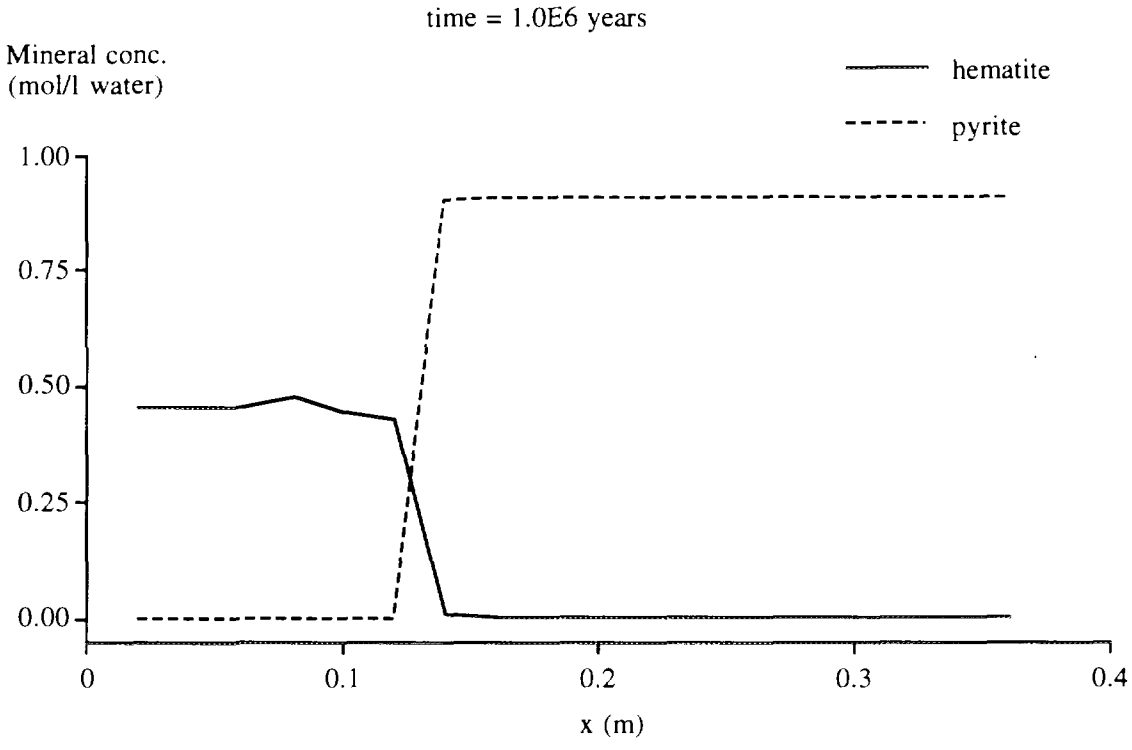


Figure 7.4.3 Concentration profiles of pyrite and hematite in the bentonite buffer $1.0 \cdot 10^6$ years after the sealing of the repository.

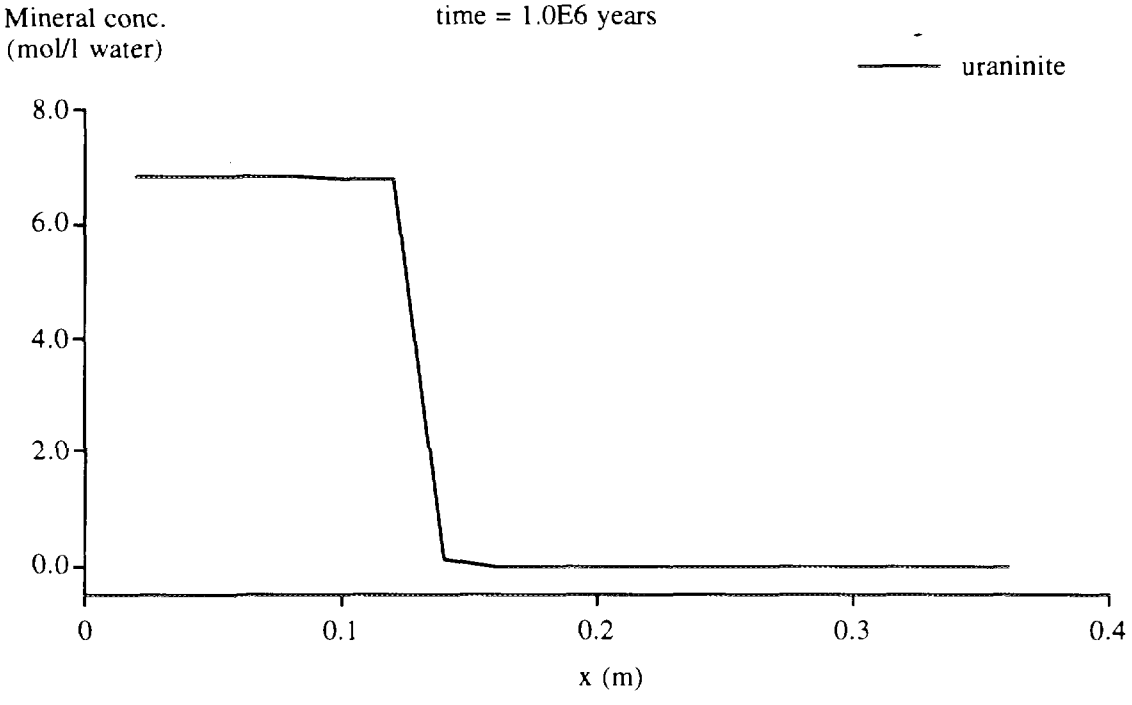


Figure 7.4.4 Concentration profile of uraninite in the bentonite buffer $1.0 \cdot 10^6$ years after the sealing of the repository.

Again the low-temperature alteration of Na-montmorillonite to illite has not occur as shown by the modelling results.

# 8 Discussions and conclusions

In this study, we try to address two mechanisms that can possibly affect the long-term properties of the bentonite buffer surrounding the canister in a final spent nuclear fuel disposal repository. The two mechanisms are the oxidation of the reducing mineral(s) in the bentonite buffer by radiolytically generated oxidants, and the low-temperature alteration of the sodium montmorillonite in the buffer to illite. Both the complete oxidation of the reducing mineral and the alteration to illite will lead to considerable increase in the release of radionuclides and fission products from the canister through the buffer to the granitic bedrock.

Four cases have been considered. Modelling results of all the four cases indicate that, under the chemical conditions of the near-field, at a temperature of 25°C or lower, Na-montmorillonite will not be converted to illite, at least up to the time $1.0 \cdot 10^6$ years after the sealing of the repository. This conclusion is in good agreement with other studies (Pytte, 1982), which concluded that at low temperatures, the montmorillonite will be stable up to $10^8$ to $10^9$ years.

Modelling results of all the four cases indicate that the pyrite in the bentonite buffer can be oxidised by the radiolytically generated oxidant. In Cases 1 and 2 of this study, the oxidant directly oxidises pyrite in the bentonite. The oxidising power is carried by the dissolved oxygen. In the zone where pyrite is oxidised, no other reducing minerals are present, and the Eh values are very high, of about 0.8 V. In the zone where pyrite has not yet been oxidised, the dissolved oxygen concentration is virtually zero. The concentration gradient of dissolved oxygen is the driving force for the mass transport of the oxidising power by diffusion. In Cases 3 and 4, the oxidant first oxidises uraninite in the spent fuel, the oxidised hexa-valent uranium in the aqueous phase is transported to the bentonite buffer to oxidise pyrite. When reacted with pyrite, the hexa-valent uranium is reduced to tetra-valent uranium, and it precipitates as uraninite in the oxidised zone in the bentonite buffer. The Eh values in the oxidised zone is about 0.2 V. The dissolved oxygen concentration is low at these Eh values. The oxidising power is now carried by the dissolved hexa-valent uranium.

In cases where there is the same amount of pyrite present in the bentonite buffer, the redox front propagates at the same rate, irrespective of whether the oxidising power is carried by the dissolved oxygen or it is carried by the hexa-valent uranium. The detailed aspects of chemistry, however, are different.

When the amount of pyrite in the buffer is 200 mg per kg of bentonite, the redox front breaks through the bentonite buffer at about 14 000 years after the sealing of the repository, under the assumptions of the present study. When the amount of pyrite is

0.76% by weight, the redox front has propagated to a distance 0.12 m from the canister, at the time of $1.0 \cdot 10^6$ years after the sealing of the repository.

It should be noted that the more realistic situation would be that part of the radiolytically generated oxidant oxidises the uraninite in the spent fuel, and the rest is transported directly to the bentonite buffer, due to the chemical kinetics of the dissolution of the spent fuel (Bruno et al., 1995). The actual geochemical conditions of the bentonite buffer would possibly be somewhere in between of Cases 1 and 2, and Cases 3 and 4.

In this study, some very important aspects of the chemical reactions between the bentonite and the porewater are not considered, such as ion-exchange reactions. Only the release of uranium is considered in this study. Release of other radionuclides has not been accounted for. In addition, the chemical reactions are assumed to be in equilibrium by the model. Detailed chemical kinetics has not been addressed. How these features can affect the conclusions of this study still needs to be invested in the future.

The conclusions of this study are as follows.

(1) The coupled mass transport with geochemical reaction models are feasible to be used to illustrate the long-term stability of the bentonite buffer.

(2) At low temperatures, the sodium montmorillonite in the bentonite buffer is chemically stable with respect to the chemical conditions of the near-field. Alteration to illite and thus an increase of hydraulic conductivity is not likely to occur.

(3) The radiolytically generated oxidant can oxidise the reducing minerals in the bentonite buffer. A redox front can be generated. In all the different cases considered in this study, the modelling results indicate that a slightly less than 1% by weight of pyrite in the bentonite buffer will be able to ensure that the redox front does not penetrate through the bentonite buffer within 1 million years.

# 9 References


Arthur R. C. and Apted M. J., 1994. SITE-94: Near-Field Chemistry. Draft Technical Report. Intera Information Technologies Inc. 3609 S. Wadsworth Blvd., 5th Floor, Denver, Colorado, 800235, USA.

Allard B., Larson S. A., Tullborg E.-L. and Wikberg P., 1983. Chemistry of deep groundwaters from granitic bedrock. KBS TR 83-59.

Andersson K., 1990. Natural variability in deep groundwater chemistry and influence on transport properties of trace radionuclides. SKI TR 90-17.

Bruno J., Cera E. and Duro L., 1995. A kinetic model for the stability of spent fuel under oxic conditions. Preliminary report. Intera, Barcelona, Spain.

Choppin G. R. and Rydberg J., 1980. *Nuclear Chemistry. Theory and Applications.* Pergamon Press.

Christensen H. and Bjergbakke E., 1982. Radiolysis of groundwater form spent fuel. SKBF/KBS Technical Report 82-18.

Cross J. E., Haworth A., Lichtner P. C., MacKenzie A. B., Moreno L., Neretnieks I., Nordstrom D. K, Read D, Romero L., Scott R. D., Sharland S. M. and Tweed C. J., ed. by McKinley I. G., 1991. Testing models of redox front migration and geochemistry at the Osamu Utsumi mine and Morro do Ferro analogue sites, Poços de Caldas, Brazil. Nagra NTB 90-30; SKB TR 90-21; UK DOE WR 90-052.

Eriksen T. and Jacobsson A., 1983. Radiation effects on the chemical environment in a radioactive waste repository. SKBF/KBS TR 83-27.

Forslind E. and Jacobsson A., 1975. *Clay-water systems. Water, a comprehensive treatise. Vol. 5.* Plenum Press.

Haworth A., Sharland S. M., Tasker P. W. and Tweed C. J., 1988. A guide to the coupled chemical equilibria and transport code CHEQMATE. Harwell Laboratory Report NSS-R113. Oxfordshire, UK.

KBS-3, 1983. Final storage of spent nuclear fuel – KBS-3. Swedish Nuclear Fuel Supply Co/Division KBS.

Liu J., 1995. *Development and Test of Models in the Natural Analogue Studies of the Cigar Lake Uranium Deposit.* Ph. D. Thesis. Department of Chemical Engineering and Technology, Royal Institute of Technology, Stockholm, Sweden.

Neretnieks I., 1995. A note on fuel dissolution. (To be published).

Neretnieks I., Yu J.-W. and Liu J., 1995. An efficient time scaling technique for coupled geochemical and transport models. *Symp. of the fifth Int. Conf. on the Chemistry and Migration Behaviour of Actinides and Fission Products in the Geosphere.* Saint. Malo, France. Sept. 10-15, 1995 (submitted to *J. Contaminant Hydrology*).

Newman A. C. D., 1987. The Interaction of Water with Clay Mineral Surfaces. In: *Chemistry of clays and clay minerals. Mineralogical Society Monograph No. 6*, Newman A. C. D. (ed.), Longman Scientific & Technical.

Newman A. C. D. and Brown G., 1987. The Chemical Constitution of Clays. In: *Chemistry of clays and clay minerals. Mineralogical Society Monograph No. 6*, Newman A. C. D. (ed.), Longman Scientific & Technical.

Parkhurst D. L., Thorstenson D. C. and Plummer L. N., 1980. PHREEQE – A computer program for geochemical calculations. US Government Report. PB 81-167801.

Pusch R., 1982. Mineral-water interactions and their influence on the physical behaviour of highly compacted Na bentonite. *Can. Geot. Journal*, vol. 19, No. 3.

Pusch R. and Börgesson L., 1992. PASS - Project on alternative systems study. Performance assessment of bentonite clay barrier in three repository concepts: VDH, KBS-3 and VLH. SKB TR 92-40.

Pusch R., Karnland O., Hökmark H., Sandén T. and Börgesson L., 1991. Final report of the Rock Sealing Project – Sealing properties and longevity of smectitic clay grouts. Stripa Project Technical Report 91-30.

Pytte A. M., 1982. *The kinetics of the smectite to illite reaction in contact metamorphic shales.* Thesis M. A., Dartmouth College, NH, USA.

Romero L., Moreno L. and Neretnieks I., 1995. Movement of a redox front around a repository for high-level nuclear waste. *Nucl. Tech.*, **110**, 238-249.

Singer P. C. and Stumm W., 1970. *Science*, **167**, 3921.

SKB 91, 1992. Final disposal of spent nuclear fuel. Importance of the bedrock for safety. SKB TR 92-20.

SKI, 1991. SKI Project-90. SKI TR 91-23.

Stumm W. and Morgan J. J., 1996. *Aquatic Chemistry. Chemical Equilibria and Rates in Natural Waters.* Third Edition. John Wiley & Sons.

Torstenfelt B., Allard B., Johansson W. and Ittner T., 1983. Iron content and reducing capacity of granites and bentonite. SKBF/KBS TR 83-36.

Wanner H., Wersin P. and Sierro N., 1992. Thermodynamic modelling of bentonite-groundwater interaction and implications for near field chemistry in a repository for spent fuel. KBS TR 92-37.

Wanner H., Albinsson Y. and Wieland E., 1994. Project caesium - An ion exchange model for the prediction of distribution coefficient of caesium in bentonite. SKB TR 94-10.

Wersin P., Spahiu K. and Bruno J., 1994. Time evolution of dissolved oxygen and redox conditions in a HLW repository. SKB TR 94-02.

Wolery T. J., 1980. *Chemical Modelling of Geologic Disposal of Nuclear Waste: Progress Report and a Perspective.* UCRL-52748. Lawrence Livermore Laboratory, Livermore, CA, USA.

Worgan K. J. and Robinson P. C., 1995. Site-94. User Guide for CALIBRE, Version 2. SKI Report 95-12.



| Postadress/Postal address | Telefon/Telephone | Telefax | Telex |
|---|---|---|---|
| SKI<br>S-106 58 STOCKHOLM | Nat 08-698 84 00<br>Int +46 8 698 84 00 | Nat 08-661 90 86<br>Int +46 8 661 90 86 | 11961 SWEATOM S |